LA-UR-15-28775 (Accepted Manuscript)

Synthesis and characterization of potassium aryl- and alkyl-substituted silylchalcogenolate ligands

Brown, Jessica Lynn
Janicke, Michael Timothy
Scott, Brian Lindley
Gaunt, Andrew James

To be published in: Dalton Transactions

DOI to publisher's version: 10.1039/C5DT04433B

Permalink to record: http://permalink.lanl.gov/object/view?what=info:lanl-repo/lareport/LA-UR-15-28775

Synthesis and Characterization of

Potassium Aryl- and Alkyl-Substituted Silylchalcogenolate Ligands

Jessie L. Brown,[a] Michael T. Janicke,[a] Brian L. Scott[b] and Andrew J. Gaunt[*,a]

[a]Chemistry Division and [b]Materials Physics and Applications Division, Los Alamos National Laboratory, Los Alamos, New Mexico 87545, USA

*To whom correspondence should be addressed. Email: gaunt@lanl.gov

Abstract

Treatment of either triphenyl(chloro)silane or *tert*-butyldiphenyl(chloro)silane with potassium metal in THF, followed by addition of 18-crown-6, affords [K(18-crown-6)][$SiPh_3$] (**1**) and [K(18-crown-6)][$SiPh_2{}^tBu$] (**2**), respectively, as the reaction products in high yield. Compounds **1** and **2** were fully characterized including by multi-nuclear NMR and IR spectroscopies. Addition of elemental chalcogen to either **1** or **2**, results in facile chalcogen insertion into the potassium-silicon bond to afford the silylchalcogenolates, [K(18-crown-6)][E–$SiPh_2$R] (E = S, R = Ph (**3**); Se, R = Ph (**4**); E = Te, R = Ph (**5**); E = S, R = ^{t}Bu (**6**); E = Se, R = ^{t}Bu (**7**); E = Te, R = ^{t}Bu (**8**)), in moderate to good yield. The silylchalcogenolates reported herein were characterized by multi-nuclear NMR and IR spectroscopies, and their solid-state molecular structures were determined by single-crystal X-ray crystallography. Importantly, the reported compounds crystallize as discrete monomers in the solid-state, a structural feature not previously observed in silylchalcogenolates, providing well-defined access routes into systematic metal complexation studies.

Introduction

Silylchalcogenolates, of the general formula $[R_3SiE]^-$ (R = alkyl, aryl; E = S, Se, Te), have wide application in a variety of chemical transformations, including stabilizing transition metal complexes,[1-13] facilitating nanocluster formation[14-16] and promoting new synthetic designs of small-molecule magnets[17]. However, despite their growing interest, investigations into their solution-phase spectroscopic signatures, and solid-state molecular structures in particular, continue to be an area with much yet to be discovered.[1,3,11,18-21] Furthermore, in comparison to the more common silylthiolates reported in the literature, synthesis, isolation and structural

characterization of the silyl-selenolate and -tellurolate derivatives remains scarce.[1] As such, we are interested in developing a series of silylchalcogenolate scaffolds that can be prepared in a facile manner, are well-defined and are poised for subsequent coordination to various metal cations and systematic electronic and bonding studies down the chalcogen donor atom group. One specific area of interest is elucidating differences between lanthanide and actinide bonding with soft donor ligands because any evidence for covalency differences that are highlighted may have implications for the understanding and design of f-element chemical separation processes.[22-24] Despite some progress, there is a lack in the number of systematic soft donor bonding studies with the f-elements to allow wide ranging comprehension of the bonding in these systems – providing a suite of easily accessed and well-characterized S, Se, and Te donor ligands, such as those detailed in this paper, will help to provide a platform to fill this knowledge gap.

A survey of the current literature demonstrates a number of synthetic methods to isolate alkali metal silanide compounds of the generic formula, $R_3Si–M$ (R = alkyl, aryl; M = alkali metal).[25] These particular compounds are well-suited precursors to silylchalcogenolates due to facile insertion of a chalcogen atom into the Si-M bond.[1,19,20] Specifically regarding the preparation of alkali metal silanides, cleavage of a disilane (i.e. R_3SiSiR_3) with either an alkali metal or alkali metal *tert*-butoxide is a common strategy.[26-37] Other synthetic procedures include reaction between a $R_3Si–H$ precursor with either an alkali metal or alkali metal hydride, the latter producing H_2 gas as a by-product; however, low yields and unwanted side reactions make these pathways less desirable.[28,38-40] Another strategy was reported by Kleeberg and co-workers, where the silylborane, Ph_3Si-B(pin) (pin = $OCMe_2CMe_2O$), was reacted with [K(18-crown-6)][^{t}BuO], resulting in activation of the Si-B bond to afford the potassium silanide salt, [K(18-crown-

6)][$SiPh_3$].[41] However, the synthesis of the silylborane is not trivial and thus, this procedure has limited practicality for isolating other silanide derivatives.[42] Lastly, in 2004, Lerner and co-workers reported the facile preparation of a series of di-*tert*-butylphenylsilanides, namely, $^tBu_2PhSi$–M (M = Li, Na, K), by reaction of di-*tert*-butylphenyl(bromo)silane, $^tBu_2PhSi$-Br, with various alkali metals.[43] This procedure was inspired by similar protocols reported for the preparation of [$Li(THF)_3$][$SiPh_2{}^tBu$][44] and [$Li(THF)_3$][$SiPh_3$].[19,45] Importantly, this latter synthetic strategy is simplistic, high yielding and transferable to a variety of commercially available or readily prepared (bromo)- and (chloro)-silanes.[43] While the preparation of silylchalcogenolates can be realized under a variety of reaction conditions,[18,46] it has been demonstrated that elemental chalcogens readily insert into the Si-M bond to afford the respective silylchalcogenolate in good to excellent yields.[1,19,20] Consequently, we have chosen a similar route for the silylchalcogenolate compounds reported herein.

In this paper, the facile preparation of a series of potassium aryl- and alkyl-substituted silylchalcogenolate salts derived from chalcogen insertion into a potassium-silicon bond is described. All compounds reported herein were characterized by multi-nuclear NMR and IR spectroscopies, including importantly, the determination of their solid-state molecular structures by single-crystal X-ray crystallography. The reported series provides a rare opportunity to understand their coordination modes in the solid-state. Furthermore, their isolation allows for systematic study of their subsequent complexation reactivity and thus, determination of any bonding trends within the series as the electronics of the ligands are synthetically modified. The results of currently ongoing investigations into the coordination chemistry of these particular chalcogen donor scaffolds with a variety of metal salts are expected to be reported in the future.

Results/Discussion

(i) Synthesis and characterization of silanide precursors.

Following a similar protocol as Lerner and co-workers[1,43] the putative silanide, $[K(THF)_n][SiPh_3]$, was prepared by addition of Ph_3Si-Cl to two equiv of potassium metal in tetrahydrofuran (THF). Attempts to isolate this product in meaningful yields proved difficult, likely due to its incredibly high solubility in THF. However, subsequent addition of 18-crown-6 to the *in situ* generated silanide, followed by recrystallization with hexanes, affords [K(18-crown-6)][$SiPh_3$] (**1**) in high yield as an orange crystalline solid (Equation 1). The synthesis and structural characterization of **1** was first reported by Kleeberg and then again more recently by the Okuda laboratory.[26,41,47] One advantage of silanide compounds is the ability to easily modify the ligand with a variety of alkyl and aryl substituents on the silicon atom depending on the desired electronic and/or steric properties of the resulting compound. In an attempt to potentially increase the solubility of any resulting transmetallation products (and also provide a suite of ligands that allows for investigation into the effect of electron-donating groups upon subsequent complexation to metal cations), we extended this same synthetic methodology with the commercially available *tert*-butyl substituted analogue of Ph_3Si-Cl, namely, $^tBuPh_2Si$-Cl. As such, the *tert*-butyl derivative, [K(18-crown-6)][$SiPh_2{}^tBu$] (**2**), was prepared in a similar fashion as **1** and isolated as a red-orange compound in high yield (Equation 1).

$$RPh_2Si\text{-}Cl \xrightarrow[\text{2. 18-crown-6}]{\text{1. 2 K}^0} [K(\text{18-crown-6})][SiPh_2R] \quad (\text{eq. 1})$$
$$\text{THF} \qquad R = Ph\ (\mathbf{1}),\ {}^tBu\ (\mathbf{2})$$

Compounds **1** and **2** were fully characterized, including by multi-nuclear NMR spectroscopy and CH elemental analysis. Notable new spectroscopic characterization

contributions include report of the silanide's IR spectra, determination of the solid-state molecular structure of the $[K(18\text{-crown-6})]^+$ salt of the *tert*-butyl derivative **2** and investigation of the silanide's stability in ambient atmosphere and general solubility properties. Specifically, both compounds **1** and **2** are very sensitive to air and water, turning to white or pale yellow colored solids upon exposure to ambient atmosphere over the course of several minutes; in solution, this color change is immediate. Compounds **1** and **2** have identical solubility properties, being extremely soluble in THF or dimethoxyethane, only partially soluble in diethyl ether or toluene and completely insoluble in hexanes. Our laboratory has also observed at least partial decomposition in acetonitrile (MeCN), where orange crystalline **1** or **2** will afford colorless solutions upon dissolution into MeCN-d_3. The resulting ^{1}H NMR spectra exhibited complicated splitting patterns with numerous overlapping resonances in the phenyl region; unfortunately, no tractable products could be isolated from the reaction mixtures (see Supporting Information). Not unexpectedly, the ^{1}H NMR spectrum of **1** in THF-d_8 is spectroscopically identical to the resonances previously reported.[26,41] The ^{1}H NMR spectrum of **2** in THF-d_8 exhibits a singlet at 0.94 ppm, assignable to the Me protons on the *tert*-butyl substituent, while the proton resonances for 18-crown-6 are observed at 3.52 ppm. Lastly, the para, meta and ortho protons of the phenyl substituents are observed as various multiplets at 6.72, 6.87 and 7.51 ppm, respectively. The $^{13}C\{^1H\}$ spectrum of **2** in THF-d_8 exhibits comparable shifts, assignable to the aryl carbon atoms, to those reported for **1**. The $^{29}Si\{^1H\}$ NMR spectrum of **2** features a single peak at 5.04 ppm (Table 1); this shift is similar to the lithiated derivative, namely, $[Li(THF)_3)][SiPh_2{}^tBu]$, which was reported to exhibit a ^{29}Si shift at 7.54 ppm in C_6D_6.[44] Lastly, compounds **1** and **2** were further characterized by IR spectroscopy (as KBr mulls) in which many of the observed features

are similar due to the mutual Si-C, C-C and C=C stretches found in both compounds (see SI for full spectral characterization of **1** and **2**).

The solid-state molecular structure of **2** was determined by X-ray crystallography (Figure 1). A summary of relevant structural parameters and full crystallographic details for compound **2** can be found in Tables 3 and 4, respectively. In the solid-state, **2** crystallizes in the monoclinic space group $P2_1/c$. It features a 4-coordinate Si center coordinated to two phenyl substituents, one *tert*-butyl substituent and one $[K(18\text{-crown-6})]^+$ cation. As expected, the bond angles about the central Si atom (C13-Si1-C19 = 99.33(3)°, C13-Si1-C25 = 102.05(3)°, C19-Si1-C25 = 106.79(3)°) indicate a distorted tetrahedral geometry. The K1-Si1 bond distance observed in **2** (3.4367(3) Å) is slightly contracted relative to the K-Si bond distance found in **1**·THF (3.460(3) Å); however, it should be noted that in the solid-state molecular structure of **1**·THF, the $[K(18\text{-crown-6})]^+$ cation is also bound to one THF molecule which may consequently skew direct comparison of the two molecule's K-Si metrics.[26] Lastly, the average Si-C bond distance in **2** (1.95(2) Å) is comparable to the metrical parameters observed in both compound **1**·THF and the lithiated derivative of **2**, namely, $[Li(THF)_3][SiPh_2{}^tBu]$.[48]

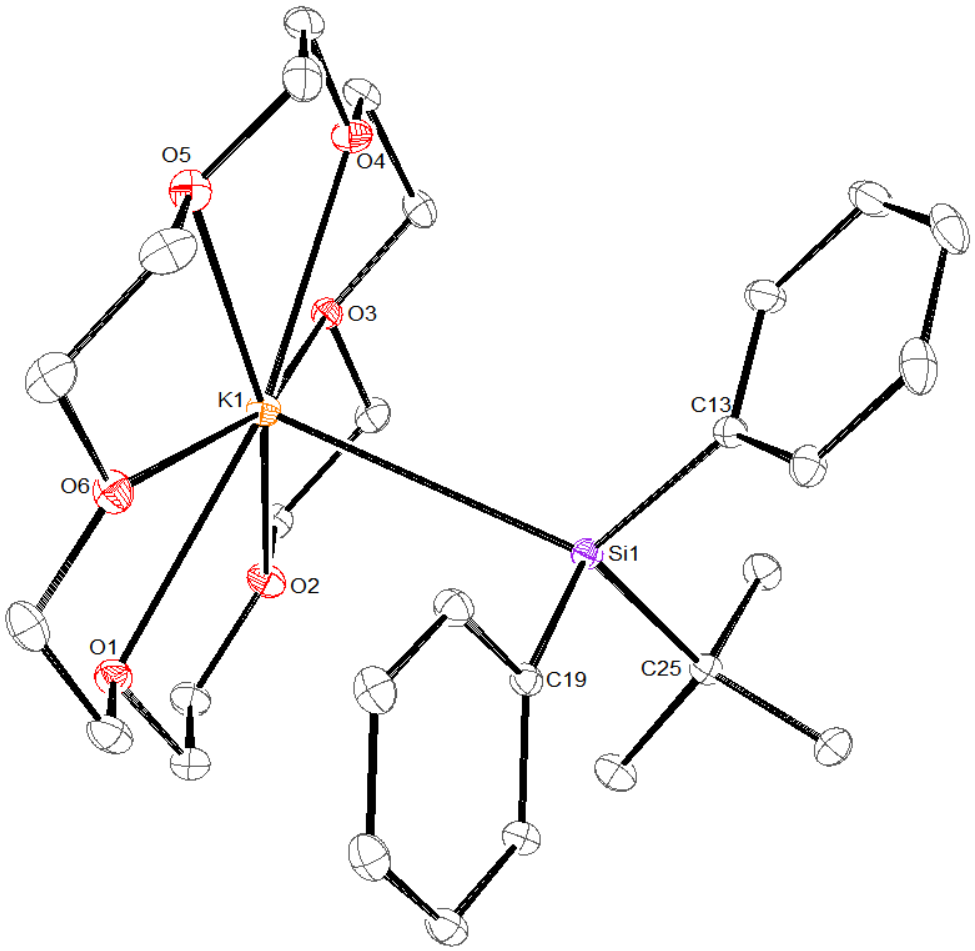

Figure 1. Solid-state molecular structure of **2** with 30 % probability ellipsoids. Hydrogen atoms omitted for clarity.

(ii) Chalcogen addition (sulfur, selenium, tellurium) to silanide precursors, 1 and 2.

$$[K(18\text{-crown-6})][SiPh_2R] \xrightarrow[\text{THF}]{E} [K(18\text{-crown-6})][E\text{-}SiPh_2R] \quad (eq.\ 2)$$

R = Ph (**1**), ^{t}Bu (**2**)

E = 0.125 S_8, Se, Te

R = Ph, E = S (**3**)
R = Ph, E = Se (**4**)
R = Ph, E = Te (**5**)
R = ^{t}Bu, E = S (**6**)
R = ^{t}Bu, E = Se (**7**)
R = ^{t}Bu, E = Te (**8**)

Previously, Lerner and co-workers have demonstrated that chalcogen insertion into a silicon-alkali metal bond proceeds in a facile manner.[1] Accordingly, addition of 1 equiv of elemental sulfur to a THF-d_8 solution of **1** results in an immediate color change and the appearance of several new resonances as observed by ^{1}H NMR spectroscopy (see SI). Specifically, the phenyl protons coalesce from three multiplets (as observed in the ^{1}H NMR spectrum of **1**) to two multiplets observed at 7.06 and 7.74 ppm, tentatively assignable to a new silylthiolate compound. Similar reactivity is observed upon addition of elemental sulfur to a THF-d_8 solution of **2** (see SI). Importantly, in both experiments evidence for the formation of unwanted side products, such as dichalcogenides or disilanes, was not observed to any appreciable extent. With these results in hand, we sought to isolate the product observed in the *in situ* ^{1}H NMR spectra. Addition of 1 equiv of sulfur to a solution of either **1** or **2** in THF, followed by crystallization from THF/hexanes affords the silylthiolates, [K(18-crown-6)][S-SiPh$_2$R] (R = Ph (**3**), ^{t}Bu (**6**)), as pure compounds in reasonable yields (Equation 2). In an analogous fashion, the selenolate and tellurolate derivatives, [K(18-crown-6)][E-SiPh$_2$R] (E = Se, R = Ph (**4**); E = Te, R = Ph (**5**); E = Se, R = ^{t}Bu (**7**); E = Te, R = ^{t}Bu (**8**)), were also prepared and isolated in good yield (Equation 2). Compounds **3**-**8** have the same solubility properties (qualitatively) as **1** and **2**, and are also very sensitive to air and water in both the solid-state and solution-phase.

Table 1. Multi-nuclear NMR resonances (in ppm) for compounds **1**-**8**.[a]

	^{1}H-ipso	^{1}H-ortho	^{1}H-meta	^{1}H-para	^{29}Si{^{1}H}	^{77}Se{^{1}H}	^{125}Te{^{1}H}
1[b]	160.95	137.20	126.46	123.10	-8.24	–	–
2	162.34	137.90	126.03	122.65	5.04	–	–
3	147.75	136.78	126.94	126.76	-7.35	–	–
4	146.87	137.07	126.95	126.72	-4.13	-547.35	–
5	145.65	137.46	126.95	126.63	-11.67	–	-1303.40

6	146.66	137.49	126.65	126.40	2.58	–	–
7	145.74	137.88	126.68	126.33	10.05	-580.75	–
8	144.78	138.41	126.72	126.26	5.52	–	-1360.10

[a]NMR spectra were recorded in THF-d_8 solutions. [b]Data taken from ref 26.

In addition to X-ray crystallography (*vide infra*), the silylchalgenolates, **3**-**8**, were characterized by multi-nuclear NMR spectroscopy; a summary of their respective NMR shifts are tabulated in Table 1. The ^{1}H and ^{13}C{^{1}H} shift values of **3**-**8** are very similar with little to no discernable trends regardless of the substituents on the Si atom or the identity of the inserted chalcogen. In contrast, the ^{29}Si{^{1}H} resonances are shifted upfield for the triphenyl derivatives, **3**-**5**, while compounds **2** and **6**-**8** have ^{29}Si{^{1}H} resonances that are further downfield, attributable to replacing an aryl substituent with a *tert*-butyl group.[1] The ^{77}Se{^{1}H} or ^{125}Te{^{1}H} NMR spectra were also recorded for compounds **4** and **7**, and **5** and **8**, respectively. As expected, there is little difference in the environment about the selenium atom in **4** and **7** and thus, the ^{77}Se{^{1}H} shift values of the two salts are similar. This is also observed for the tellurolate derivatives, **5** and **8**. Importantly, the compounds exhibit comparable ^{77}Se{^{1}H} and ^{125}Te{^{1}H} NMR shift values to those reported for other silylchalcogenolates and disilyldichalcogenides.[1,20] IR spectroscopy of **3**-**8** (as KBr mulls) provide fingerprint spectra.

Table 2. Selected bond distances (Å) and bond angles (deg) for compounds **3**·0.5THF, **4**·THF and **5**·THF, the 'E–$SiPh_3$' (E = S, Se, Te) ligands.*

	3·0.5THF	**4**·THF	**5**·THF
Si–E	2.039(2)	2.1893(3)	2.4210(6)
$Si–C_{av.}$	1.887(3)	1.891(1)	1.892(2)
E–K	3.143(2)	3.3506(3)	3.5832(6)
$K–O_{av.(18\text{-}C\text{-}6)}$	2.83(9)	2.82(6)	2.82(7)
$K–O_{(THF)}$	-	2.7998(9)	2.7917(13)
Si–E–K	107.03(5)	105.236(9)	101.588(12)

*The error in the average bond lengths is equal to the standard deviation in the experimental values. For **3**, no K–O distance is reported because disorder meant that the THF molecule was accounted for using the 'squeeze' methodology.

Table 3. Selected bond distances (Å) and bond angles (deg.) for compound **2**, the silanide precursor, and **6**·0.5THF, **7**·0.5THF and **8**·0.5THF, the 'E–$SiPh_2{}^tBu$' (E = S, Se, Te) ligands.*

	2	**6**·0.5THF	**7**·0.5THF	**8**·0.5THF$_{solvate}$	**8**·0.5THF$_{non\text{-}solvate}$
Si–K	3.4367(3)	–	–	–	–
Si–$E_{av.}$	–	2.054(2)	2.1943(6)	2.440(3)	
Si–$C_{av.}$	1.95(2)	1.91(1)	1.91(1)	1.91(1)	1.903(9)
E–$K_{av.}$	–	3.20(6)	3.29(5)	3.467(7)	
K–$O_{av.(18\text{-}C\text{-}6)}$	2.82(6)	2.84(5)	2.83(5)	2.81(4)	2.84(6)
K–$O_{(THF)}$		–	–	2.7355(16)	–
Si–E–K	–	112.36(3), 110.59(3)	110.669(19), 108.228(19)	107.826(14)	98.165(14)

*The error in the average bond lengths is equal to the standard deviation in the experimental values. Compounds **6, 7,** and **8** all contain two crystallographically independent molecules in the unit cell, but only in the solid-state molecular structure of compound **8** were the exact metrical parameters of an associated 0.5 THF molecule ascertained (it is bound to one K cation of one of the independent molecules in the unit cell while the other independent molecule is solvent free). In the solid-state molecular structures of compounds **6** and **7**, the 0.5 THF molecule was disordered and the electron density accounted for using the 'squeeze' methodology.

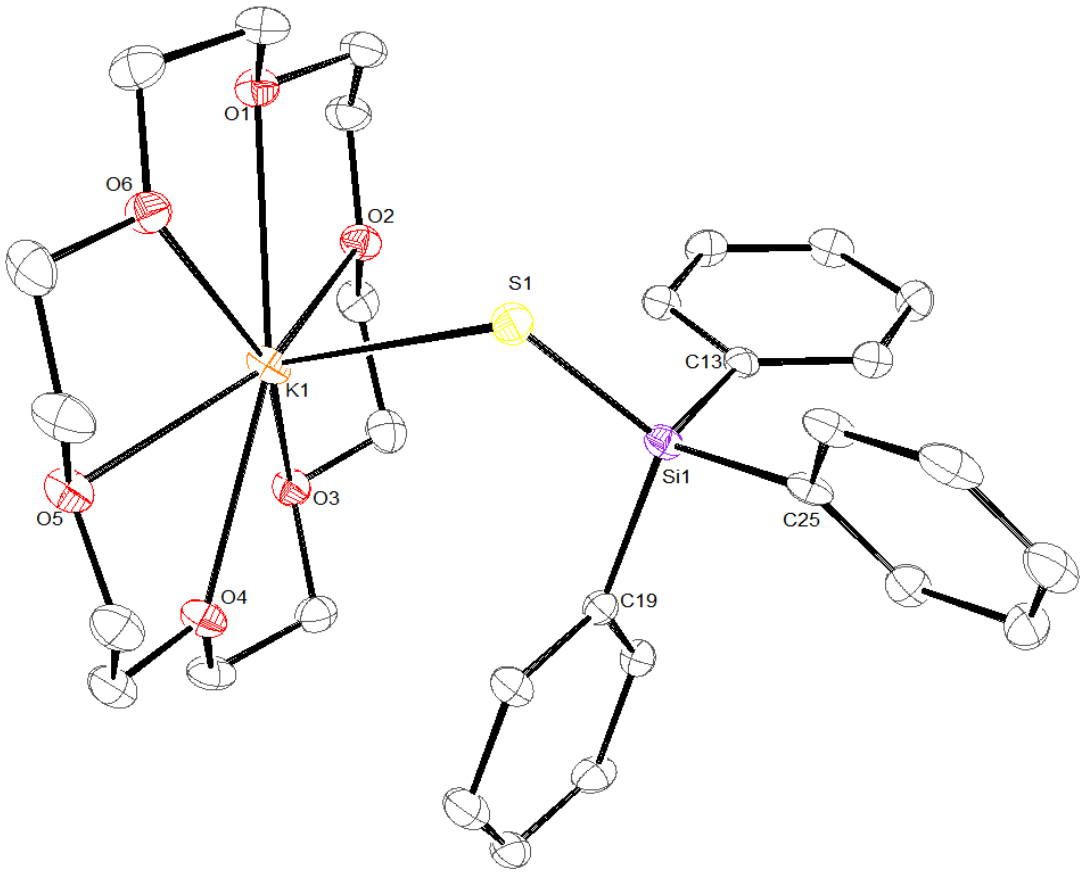

Figure 2. Solid-state molecular structure of **3** with 30 % probability ellipsoids. Hydrogen atoms omitted for clarity.

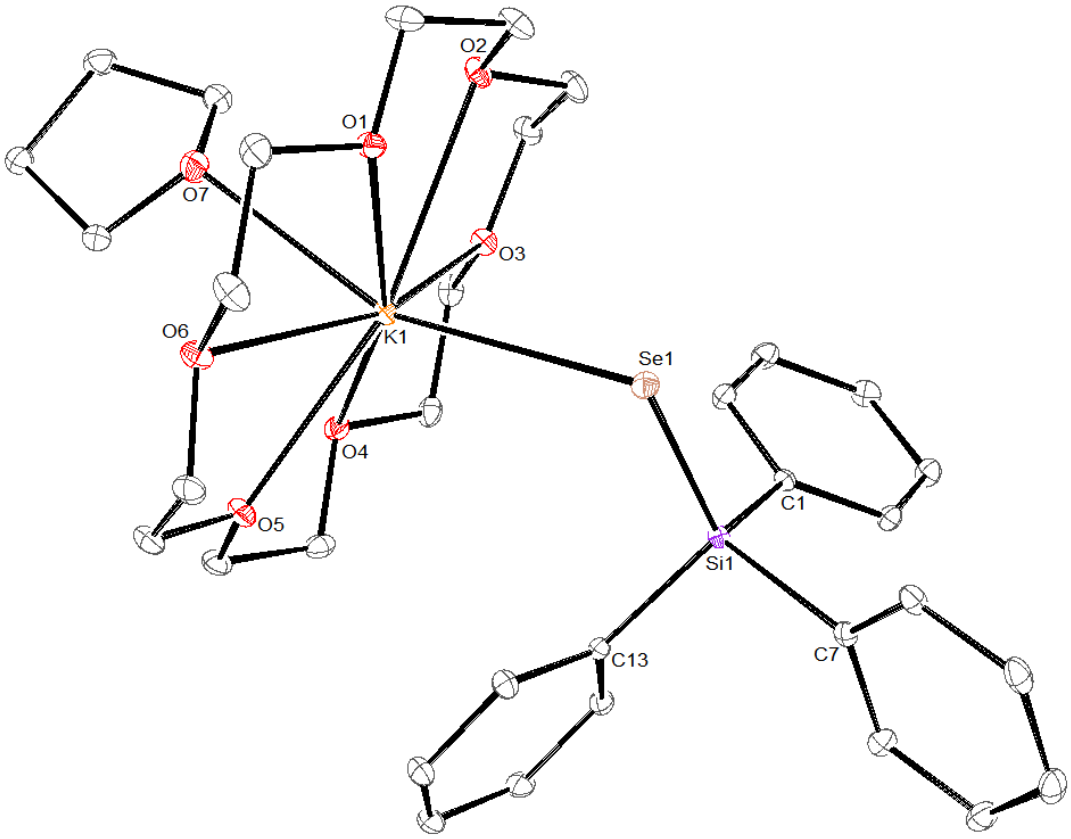

Figure 3. Solid-state molecular structure of **4** with 30 % probability ellipsoids. Hydrogen atoms omitted for clarity.

Despite the rather common use of triphenylsilylchalcogenolates, and derivatives thereof, in complexation reactivity, structural information on the ligands themselves is rather limited.[1,3,18,46] As such, compounds **3**-**8** were also structurally characterized by single-crystal X-ray crystallography in order to fully understand their coordination chemistry in the solid-state and to discern any observable bonding trends within the series, and serve as a well-defined platform for future systematic metal complexation reactions. The solid-state molecular structures of compounds **3**-**8** are shown in Figures 2-7. A summary of selected structural parameters for compounds **3**-**5** and **6**-**8** can be found in Tables 2 and 3, respectively, while their full crystallographic details can be found in Table 4.

[K(18-crown-6)][S-$SiPh_3$] (**3**) crystallizes in the triclinic space group P-1 and its solid-state molecular structure is shown in Figure 2. It contains 0.5 disordered THF molecules associated with the molecular formula for one ligand molecule which were accounted for by employing PLATON 'SQUEEZE' protocols (see SI).[49] Not unexpectedly, **3**·0.5THF features a four-coordinate silicon center bonded to three phenyl substituents and one sulfur atom in a nearly ideal tetrahedral geometry (C25–Si1–C19 = 103.81(15)°; C25–Si1–C13 = 106.81(15)°; C19–Si1–C13 = 106.17(15)°). The average Si–C bond distance (1.887(3) Å) is typical of these compounds; specifically, it is statistically identical to the average Si–C bond distance (1.890(6) Å) in the hexameric sodium thiolate, $[NaS(SiPh_3)]_6(toluene)_2$.[18] Interestingly, the Si1–S1 bond distance (2.039(2) Å) is contracted relative to other structurally characterized silylthiolates; $[(TMEDA)LiSSiMe_2{}^tBu]_2$ (2.079(1) Å, TMEDA = *N*,*N*,*N'*,*N'*-tetramethylethylenediamine),[46] $[(THF)_2NaSSi{}^tBu_3]_2$ (2.086(2) Å),[1] $[NaSSiPh_3)]_6(toluene)_2$ (2.085(5) Å),[18] and $[Na(THF)SSiPh{}^tBu_2]_4$ (2.0846(17) Å)[3]. However, the presence of the $[K(18\text{-crown-6})]^+$ cation in **3**·0.5THF and the observation that it crystallizes as a discrete monomer may effect direct comparison to the previously reported multimeric lithium and sodium silylthiolates salts. Importantly, compound **3**·0.5THF is a rare example of a structurally characterized potassium silylthiolate compound, exhibiting a S1–K1 bond distance of 3.143(2) Å in the solid-state. The K–S–Si moiety in **3**·0.5THF deviates significantly from linearity exhibiting a K1–S1–Si1 bond angle of 107.03(5)°. The only other structurally characterized silylchalcogenolates reported crystallize as either dimeric or cluster structures, and thus direct comparison to the K1–S1–Si1 bond angle observed in **3**·0.5THF is not appropriate.[1,3,11,18] However, Ruhlandt-Senge and co-workers reported several monomeric triphenylmethanethiolate salts which exhibit M-S-C (M = Li, K) bond angles in the solid-state that are comparable to **3**·0.5THF. For example, the lithium

salt, [Li(15-crown-5)][S-CPh_3] features a Li1–S1–C1 bond angle of 117.60(10)°, while the potassium salt, [K(18-crown-6)][(S-CPh_3)$(THF)_{0.5}$], features a K1–S1–C1 bond angle of 112.8(2)°.[18] The authors claim the obtuse angles are a consequence of a combination of the alkali metal-crown oxygen coordination, the cation's displacement above the crown plane and the steric bulk from the phenyl substituents. Such conclusions are also reasonable explanations for the observed K1–S1–Si1 bond angle in compound **3**·0.5THF. Lastly, the average K1–O bond distance observed in the $[K(18\text{-crown-6})]^+$ cation in **3**·0.5THF (2.83(9) Å) is typical.[26,50,51]

The characterization of **3**·0.5THF by multi-nuclear NMR and IR spectroscopies, including determination of its solid-state molecule structure, represents a well-defined example of a potassium silylchalcogenolate salt. Due to the paucity of structurally characterized silylchalcogenolates containing the larger chalcogens (i.e. Se, Te)[3], and to determine any structural trends as the chalcogens are descended, we sought to extend this structural analysis to the other silylchalcogenolate molecules we have isolated. Thus, single-crystals of both the selenolate- and tellurolate-triphenylsilyl derivatives, **4** and **5**, were also examined by X-ray crystallography. [(THF)K(18-crown-6)][Se-$SiPh_3$] (**4**) crystallizes in the triclinic space group P-1 as a THF solvate (in contrast to **3**·0.5THF, the exact position of the THF molecule was determined and the O atom is bound to the K ion with a typical K–O distance of 2.7998(9) Å).[26] The solid-state molecular structure of **4**·THF is shown in Figure 3. The average Si–C bond distance (1.891(1) Å) is statistically identical to the average Si–C bond distance (1.887(3) Å) observed in **3**·0.5THF. The Si1–Se1 bond distance (2.1893(3) Å) in **4**·THF is elongated relative to **3**·0.5THF, as expected, due to the larger chalcogen. However, it is slightly contracted relative to the only other silylselenolates structurally characterized, namely, the dimeric complexes, $[(THF)_2NaSeSiR^tBu_2]_2$ (R = ^{t}Bu, Si–Se = 2.2364(6) Å; Ph, Si–Se = 2.228(4) Å).[1] However, this

observed structural difference is likely due to the bridging nature of the selenolato ligands in these particular dimeric molecules and thus, their Si–Se bond distances are elongated relative to **4**·THF. The Se–K bond distance (3.3506(3) Å) is elongated relative to **3**·0.5THF (3.143(2) Å), again likely attributable to the larger selenium atom. As observed in compound **3**·0.5THF, the K1–Se1–Si1 bond angle of 105.236(9)° in **4**·THF is also non-linear. Not unexpectedly, the average K1–O bond distance (2.82(6) Å) pertaining to the interactions with the O atoms of the 18-crown-6 ring in **4**·THF is identical to average value for the same interactions in **3**·0.5THF.

The analogous tellurolate salt, [(THF)K(18-crown-6)][Te-$SiPh_3$] (**5**), is isostructural with **4** (with the THF solvent bound to the K cation) and exhibits a K–O distance of 2.7917(13) Å. It's solid-state molecular structure is shown in Figure 4. The K–Te interaction distance in **4** is at 3.5832(6) Å and follows the trend of increasing K–E distances down the S, Se, Te group. The Te–Si distance in **5** of 2.4210(6) Å also follows an expected trend of increasing E–Si distances down the chalcogen group compared to those in **3** and **4**. However, the Te–Si is shorter than the 2.4654(7) Å distance found in only other single-crystal structural characterization of a silyltellurolate anion (in starting material form), whose formula is $[(THF)_2NaTeSiR^tBu_2]_2$, and exists in bridged dimeric form in the solid-state – a property that may account for the longer Te–Si bond.[1] The average Si–C in **5** is 1.892(2) Å, is statistically identical to those in **3** and **4**.

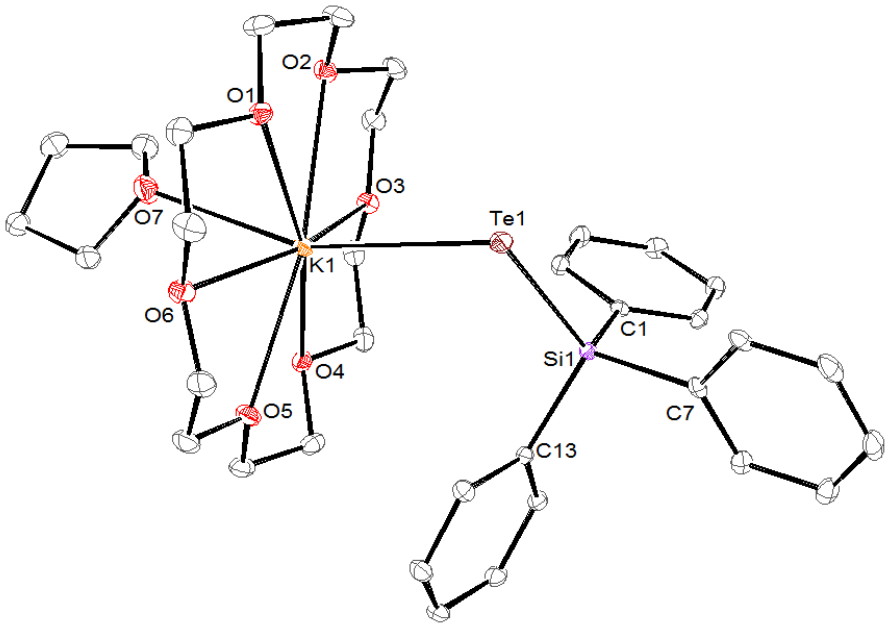

Figure 4. Solid-state molecular structure of **5** with 30 % probability ellipsoids. Hydrogen atoms omitted for clarity.

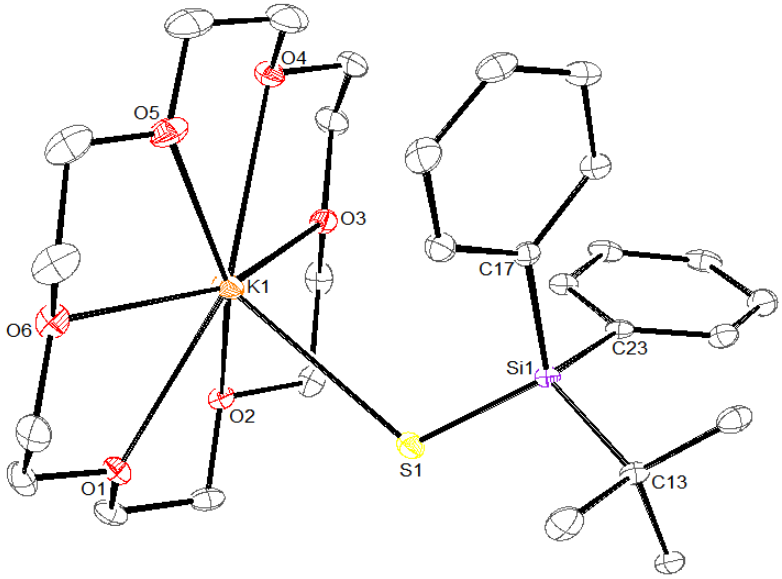

Figure 5. Solid-state molecular structure of **6** with 30 % probability ellipsoids. The second independent molecule in the unit cell and hydrogen atoms are omitted for clarity.

In an attempt to discern any further structural trends observed when one of the phenyl rings on the aryl substituent is exchanged for an alkyl group, [K(18-crown-6)][E-SiPh$_2$^{t}Bu] (E = S(**6**), Se(**7**), Te(**8**)) were also structurally characterized by X-ray crystallography. As such, their solid-state molecular structures are shown in Figures 5-7. Compounds **6** and **7** are isostructural, crystallizing in the monoclinic space group P2/n, where the asymmetric unit contains two independent monomeric molecules and the bond distances from both independent molecules have been averaged (except where noted) for the purpose of structural analysis and comparison. The average Si–C bond distances in **6**·0.5THF (1.91(1) Å) and **7**·0.5THF (1.91(1) Å) are identical and are also statistically equivalent to the Si–C distances in **3**·0.5THF and **4**·THF, demonstrating that there is little influence imparted in the Si–C bonds as a function of changing the chalcogen atom from S to Se or replacing one phenyl ring with a ^{t}Bu substituent. The average Si–E bond distance found in **6**·0.5THF (2.054(2) Å) is elongated relative to **3**·0.5THF (2.039(2) Å) but the difference is very small. This is also the case for the average Si–Se bond distance observed in **7**·0.5THF (2.1943(6) Å) which is slightly elongated relative to the Si–Se bond distance in **4**·THF (2.1893(3) Å). As expected, the average Si–Se bond distance observed in **7**·0.5THF is elongated relative to **6**·0.5THF, again due to the larger chalcogen atom. Not surprisingly, the average K–O$_{(18\text{-crown-6})}$ bond distance in **6**·0.5THF (2.84(5) Å) and **7**·0.5THF (2.83(5) Å) are statistically equivalent to one another and to the average K–O$_{(18\text{-crown-6})}$ bond distances observed in **3**·0.5THF and **4**·THF. Due to the large standard deviations associated with the average E–K bond distances in **6**·0.5THF (E = S; 3.20(6) Å) and **7**·0.5THF (E = Se; 3.29(5) Å), they are statistically identical despite Δ = 0.09 Å; thus, no meaningful conclusions on their metrical trends can be drawn. Finally, both **6**·0.5THF and **7**·0.5THF exhibit two non-linear Si–E–K bond angles (because there are two independent molecules in the unit cell). The two values

are significantly different between the independent molecules within each structure (112.36(3)° and 110.59(3)° in **6**; 110.669(19)° and 108.228(19)° in **7**) but comparing each value to the corresponding value between isostructural **6**·0.5THF and **7**·0.5THF is consistent with the trend of a slight decrease in Si–E–K bond angles down the chalcogen group. These Si–E–K angles appear larger than those in **3**·0.5THF and **4**·THF (the R = Ph_3 ligands) but the very large standard deviation associated with the average Si–E–K values in **6** and **7** prevent statistical comparison.

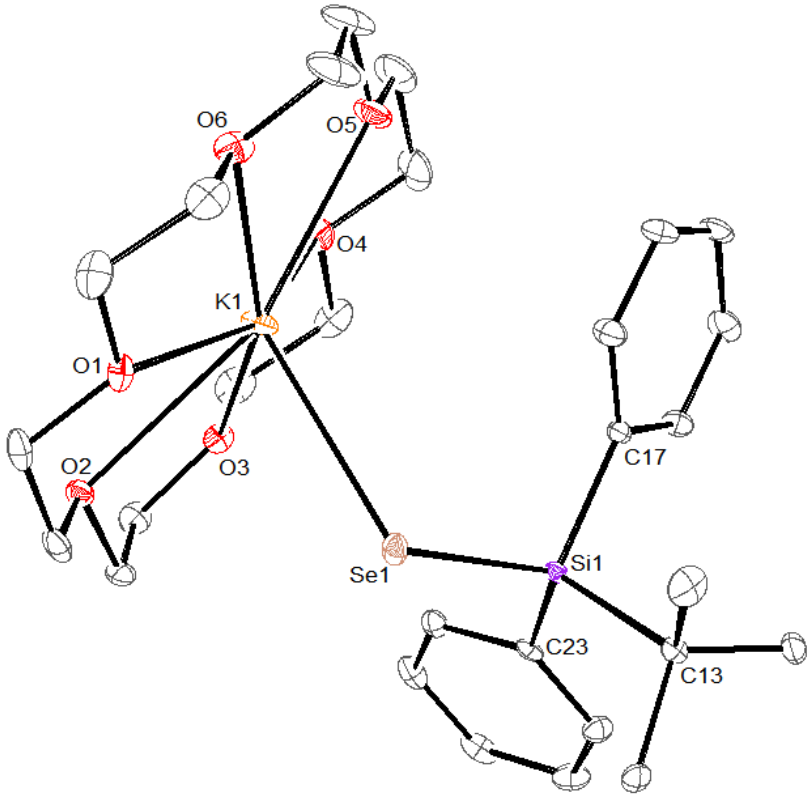

Figure 6. Solid-state molecular structure of **7** with 30 % probability ellipsoids. The second independent molecule in the unit cell and hydrogen atoms are omitted for clarity.

Compound **8** crystallizes in the orthorhombic space group $P2_12_12_1$, where the asymmetric unit contains two independent molecules. In contrast to **6**·0.5THF and **7**·0.5THF, the two molecules are not chemically equivalent. Specifically, one molecule features coordination to an oxygen atom of the THF molecule via the K atom of the $[K(18\text{-crown-6})]^+$ cation with a K–O distance of 2.7355(16) Å (Figure 7). The second molecule is unsolvated (Figure 7) with the closest potential C–H interaction of the THF molecules to the K atom exhibiting a K–C distance of over 3.4 Å, which is too long for us to assign as an agostic interaction, but it is worth noting that the orientation of the two independent molecules with respect to each other in **8** is very different to the relative orientation observed in **6** and **7** (although this may simply be an effect of the different steric properties imparted by the presence of a THF molecule). The independent molecule that is THF solvated, [(THF)K(18-crown-6)][Te-$SiPh_2{}^tBu$], features an average Si2–C bond distance (1.91(1) Å) that is comparable to the other solid-state structures already described, indicating that the alkyl/aryl substituents have little effect on the overall metrics of these particular compounds. Due to the larger Te atom, the Si2–Te2 bond distance (2.4417(5) Å) and the K2–Te2 bond distance (3.4616(4) Å) are significantly longer than those same bonds in **6**·0.5THF and **7**·0.5THF. In comparison to the Si–Te bond in **5**·THF, the Si2–Te2 bond distance in [(THF)K(18-crown-6)][Te-$SiPh_2{}^tBu$] is slightly longer, but in comparison to the only other structurally characterized silyltellurolate (in ligand form), namely, $[(THF)_2NaTeSiR^tBu_2]_2$ (Si–Te = 2.4654(7) Å) it is slightly shorter.[1] As expected the average K–O bond distance (2.81(4) Å) in the $[K(18\text{-crown-6})]^+$ cation is equivalent to the other molecules already discussed. Lastly, as observed in the previous solid-state structures described thus far, the Si2–Te2–K2 bond angle (107.826(14)°) is also non-linear. The unsolvated molecule in the asymmetric unit, namely, [K(18-crown-6)][Te-$SiPh_2{}^tBu$], features an Si1-Te1 bond distance of 2.4373(5) Å that is slightly

shorter relative to the Si2–Te2 bond of the THF solvate, attributable to the absence of a THF molecule in this portion of the solid-state structure. In contrast, the Te1–K1 bond distance of 3.4715(5) Å is longer relative to the Te2–K2 bond in the THF solvate. The average Si–C bond distance (1.903(9) Å) and the average K-O bond distance (2.84(6) Å) in the $[K(18\text{-crown-6})]^+$ cation are statistically equivalent to the THF solvate portion of the solid-state structure and to the other previously described structures. Interestingly, the Si1–Te1–K1 bond angle of 98.165(14)° is the most acute of all the Si–E–K bond angles observed in the reported series.

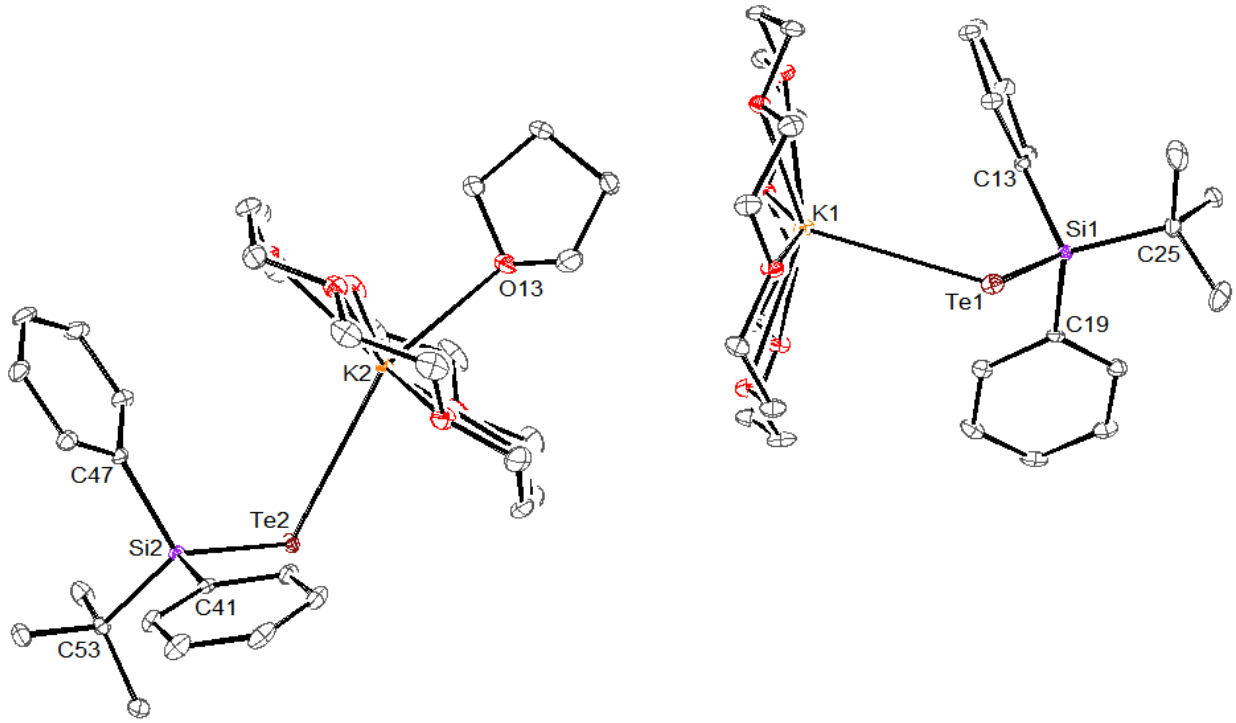

Figure 7. Solid-state molecular structure of **8** with 30 % probability ellipsoids. Both independent molecules in the asymmetric unit are shown (THF-solvate and THF-unsolvated). Hydrogen atoms removed for clarity.

Table 4. Selected X-ray Crystallographic Data for Compounds **2-8**.

	2·THF	**3**·0.5THF	**4**·THF	**5**·THF	**6**·0.5THF	**7**·0.5THF	**8**·0.5THF
Empirical formula	$C_{28}H_{43}KO_6Si$	$C_{32}H_{43}KO_{6.5}SSi$	$C_{34}H_{47}KO_7SeSi$	$C_{34}H_{47}KO_7SiTe$	$C_{30}H_{47}KO_{6.5}SSi$	$C_{30}H_{47}KO_{6.5}SeSi$	$C_{30}H_{47}KO_{6.5}SiTe$
Crystal Habit, color	plate, pale orange	plate, pale blue	slab, pale yellow	block, pale pink-red	plate, pale blue	plate, pale yellow	block, pale purple
Crystal size (mm)	0.32 × 0.14 × 0.12	0.30 × 0.20 × 0.04	0.26 × 0.14 × 0.10	0.42 × 0.34 × 0.22	0.36 × 0.13 × 0.02	0.81 × 0.49 × 0.16	0.48 × 0.24 × 0.14
Crystal system	triclinic	triclinic	triclinic	triclinic	monoclinic	monoclinic	orthorhombic
Space group	$P2_{1/c}$	P-1	P-1	P-1	P2/n	P2/n	$P2_12_12_1$
Volume ($Å^3$)	2964.9(5)	1683(2)	1761.15(17)	1820.0(6)	6493(2)	6549.7(7)	6706.4(8)
a (Å)	9.6776(9)	9.188(8)	9.2695(5)	9.2562(19)	25.991(6)	26.2187(15)	16.0831(11)
b (Å)	16.8062(15)	10.473(9)	10.3732(6)	10.431(2)	9.800(2)	9.7757(6)	19.0939(14)
c (Å)	18.2542(17)	17.685(14)	18.6978(11)	19.332(4)	26.079(6)	26.2094(15)	21.8387(15)
α(°)	90.00	95.930(9)	98.7616(12)	99.814(2)	90.00	90.00	90.00
β(°)	92.9686(17)	93.438(9)	93.9586(12)	93.297(2)	102.188(3)	102.8380(10)	90.00
γ(°)	90.00	94.815(9)	95.8326(12)	96.939(2)	90.00	90.00	90.00
Z	4	2	2	2	8	8	8
Formula weight (g/mol)	542.81	630.91	713.87	762.50	610.93	657.83	706.47
Density (calculated) (Mg/m^3)	1.216	1.245	1.346	1.391	1.250	1.334	1.399
Absorption coefficient (mm^{-1})	0.257	0.297	1.263	1.007	0.305	1.350	1.086
Total reflections	69399	16688	37364	21415	62353	81128	124291
Independent reflections	12708	6366	12746	8616	11888	12444	19420
R_{int}	0.0241	0.0774	0.0284	0.0191	0.0501	0.0437	0.0414
Final R indices [$I > 2\sigma(I)$]	R_1 = 0.0310, wR_2 = 0.0991	R_1 = 0.0564, wR_2 = 0.1339	R_1 = 0.0295, wR_2 = 0.0665	R_1 = 0.0231, wR_2 = 0.0571	R_1 = 0.0396, wR_2 = 0.0892	R_1 = 0.0332, wR_2 = 0.1033	R_1 = 0.0252, wR_2 = 0.0580

Summary

Addition of either Ph_3Si-Cl or $^tBuPh_2Si$-Cl to potassium metal in tetrahydrofuran, followed by addition of 18-crown-6, results in isolation of the silanide salts, [K(18-crown-6)][$SiPh_2R$] (R = Ph, ^{t}Bu), in high yield. The silylchalcogenolate derivatives of the general formula, [K(18-crown-6)][E-$SiPh_2R$] (E = S, Se, Te; R = Ph, ^{t}Bu), were prepared by facile insertion of the chalcogen atom into the potassium-silicon bond. The resulting compounds are well-defined, isolated in moderate to high yields and were characterized by multi-nuclear NMR and IR spectroscopies. Determination of their solid-state molecular structures by X-ray crystallography indicates the compounds crystallize as monomers, a structural feature not previously observed for silylchalcogenolates. Importantly, the reported compounds are poised for systematic complexation studies with various metal salts; such studies are currently ongoing in our laboratory. Replacement of one of the three phenyl rings with a ^{t}Bu substituent will allow steric considerations to be explored, and preliminary scoping reactions with lanthanide cations suggest that the solubility of resultant metal complexes and the conditions that favor isolation are markedly different between the R = Ph_3 and R = $Ph_3{}^tBu$ ligand variants, potentially providing multiple and flexible synthetic pathways to facilitate the pursuit of a suite of metal complexes for comparative purposes.

Experimental

General. All reactions and subsequent manipulations were performed in an inert atmosphere glove box under high purity argon gas. Diethyl ether (Et_2O), hexanes and tetrahydrofuran (THF) were purchased anhydrous from Sigma-Aldrich and stored over activated 4 Å molecular sieves for at least 48-72 h before use. THF-d_8 was dried over activated 4 Å molecular sieves for at least

48 h before use. Potassium metal was washed with a large excess of hexanes to remove the mineral oil and subsequently dried in vacuo for several hours before use. All other reagents were purchased from commercial suppliers and used as received.

NMR spectra were recorded on a Bruker Avance 400 MHz spectrometer. ^{1}H and $^{13}C\{^{1}H\}$ NMR spectra were referenced to external $SiMe_4$ using the residual protio solvent peaks as internal standards (^{1}H NMR experiments) or the characteristic resonances of the solvent nuclei (^{13}C NMR experiments). $^{29}Si\{^{1}H\}$ spectra were referenced to an external $SiMe_4$ solution (neat) before every experiment. $^{77}Se\{^{1}H\}$ spectra were indirectly referenced to Me_2Se at 0 ppm by direct reference to Ph_2Se_2 (in C_6D_6, 1 M solution) at 460 ppm.[52] $^{125}Te\{^{1}H\}$ spectra were indirectly referenced to Me_2Te at 0 ppm by direct reference to Ph_2Te_2 (in C_6D_6, 2 M solution) at 422 ppm.[52] IR spectra were recorded on a Perkin Elmer FTIR spectrometer as KBr mulls. Elemental analyses for compounds **2-8** were performed by the Midwest Microlab, LLC. (Indianapolis, IN).

Synthesis of [K(18-crown-6)][$SiPh_3$] (1). To a stirring suspension of potassium metal (54.1 mg, 1.38 mmol) in THF (3 mL) was added, dropwise, a colorless THF (5 mL) solution of Ph_3SiCl (195.2 mg, 0.66 mmol). Within minutes (<15) the solution became heavily particulated and took on the appearance of a white suspension. Over the course of several hours, the solution slowly turned to a dark yellow-green color. Following stirring at ambient temperature for ~19 h, the dark green solution was filtered through a Celite column (0.5 cm × 2 cm) supported on glass wool to give a dark orange filtrate and a small green-colored plug. The green material was never characterized and was discarded. To the orange filtrate was added 18-crown-6 (176.5 mg, 0.67 mmol) as a white solid. No color change was observed with the addition. The solution was allowed to stir at ambient temperature for ~1 h and then subsequently filtered through a Celite column (0.5 cm × 2 cm) supported on glass wool to give a deep orange filtrate. The orange

filtrate was concentrated in vacuo to ~4 mL, layered with hexanes (~6 mL) and placed in the glove box freezer at -35°C. Orange crystals and orange micro-crystalline material deposited from solution overnight and the material was dried in vacuo before use (325 mg, 87 %). ^{1}H NMR (THF-d_8, 26 ºC, 400 MHz): δ 3.51 (s, 24 H, 18-crown-6), 6.74 (t, 3 H, J_{HH} = 7.2 Hz, para CH), 6.88 (t, 6 H, J_{HH} = 7.4 Hz, meta CH), 7.37 (d, 6 H, J_{HH} = 6.5 Hz, ortho CH). By ^{1}H NMR spectroscopy, the material is spectroscopically identical to previous reports.[26,41] IR (KBr pellet, cm^{-1}): 3147(w), 3130(w), 3113(w), 3061(m sh), 3048(m), 2991(w), 2992(w), 2973(w), 2946(m sh), 2895(s), 2861(s sh), 2825(m), 2795(w sh), 2743(w), 2713(w), 2688(w), 1597(w sh), 1584(w sh), 1573(m), 1562(w sh), 1489(w sh), 1472(s), 1452(m), 1427(s), 1351(s), 1299(w sh), 1285(m), 1250(s), 1182(w), 1117(s), 1058(w sh), 1044(s), 1023(m), 997(m), 963(s), 883(w sh), 839(m), 804(w sh), 741(m), 704(s), 618(w), 549(w sh), 517(s), 495(m sh), 481(w sh), 447(w sh), 431(w).

Synthesis of [K(18-crown-6)][SiPh$_2$^{t}Bu] (2). To a stirring suspension of potassium metal (128.4 mg, 3.28 mmol) in THF (3 mL) was added, dropwise, a colorless THF (5 mL) solution of ^{t}BuPh$_2$SiCl (0.40 mL, 1.50 mmol). The solution slowly turned to a dark orange-brown color over the course of several hours. Following stirring at ambient temperature overnight (~12 h), the deep orange solution was filtered through a Celite column (0.5 cm × 2 cm) supported on glass wool to give a dark orange filtrate. To the orange filtrate was added 18-crown-6 (406.6 mg, 1.53 mmol) as a white solid. A slight color change to red-orange was observed with the addition. The solution was allowed to stir at ambient temperature for ~1 h and then subsequently filtered through a Celite column (0.5 cm × 2 cm) supported on glass wool to give a deep red-orange filtrate. The filtrate was concentrated in vacuo to ~4 mL, layered with hexanes (~10 mL) and placed in the glove box freezer at -35 °C. Red-orange crystals and micro-crystalline material

deposited from solution overnight and the material was dried in vacuo before use (769.9 mg, 92 %). Crystals suitable for X-ray analysis were grown overnight at -35°C from a THF/hexane (1:2) layered solution. Anal. Calcd for $C_{28}H_{43}K_1O_6Si_1$: C, 61.95; H, 7.98 Found: C, 61.57; H, 7.91. ^{1}H NMR (THF-d_8, 21 ºC, 400 MHz): δ 0.94 (s, 9 H, Me), 3.52 (s, 24 H, 18-crown-6), 6.72 (t, 3 H, J_{HH} = 7.2 Hz, para CH), 6.87 (t, 6 H, J_{HH} = 7.3 Hz, meta CH), 7.51 (d, 6 H, J_{HH} = 7.2 Hz, ortho CH). ^{13}C{^{1}H} NMR (THF-d_8, 21 ºC, 100 MHz): δ 20.89 (C(CH$_3$)$_3$), 32.49 (C(CH$_3$)$_3$), 71.03 (18-crown-6), 122.65 (*para*-Ph), 126.03 (*meta*-Ph), 137.90 (*ortho*-Ph), 162.34 (*ipso*-Ph). ^{29}Si{^{1}H} NMR (THF-d_8, 23 ºC, 79.5 MHz): δ 5.04 (s, K*Si*). IR (KBr pellet, cm^{-1}): 3144(w), 3114(w), 3059(m), 3042(w), 2988(w sh), 2984(w), 2947(s), 2898(s), 2881(s sh), 2820(s), 2788(w sh), 2742(w), 2709(w), 2682(w), 1977(w), 1572(m), 1552(w), 1471(m), 1453(m), 1426(m), 1376(w sh), 1349(s), 1282(m), 1247(m), 1235(m sh), 1116(s), 1056(m sh), 1040(m sh), 1024(m sh), 1008(w sh), 963(s), 837(m), 813(m), 734(m), 705(s), 682(w sh), 597(w), 557(w), 529(w sh), 509(m), 491(m), 482(m sh), 431(w).

Synthesis of [K(18-crown-6)][S-SiPh$_3$] (3). To a stirring, orange solution of [K(18-crown-6)][SiPh$_3$] (**1**) (123.1 mg, 0.22 mmol) in THF (2 mL) was added 0.125 equiv of S_8 (7.1 mg, 0.028 mmol). An immediate color change to blue was observed. Following stirring at ambient temperature for ~15 min, the solution was filtered through a Celite column (0.5 cm × 2 cm) supported on glass wool, layered with hexanes (~6 mL) and placed in the glove box freezer at -35 °C. Pale blue, almost colorless, crystals deposited from solution overnight. The crystals were isolated by decanting off the colorless supernatant. The crystals were immediately re-dissolved in THF (~2.5 mL) and allowed to stir at ambient temperature for ~15 min before the solution was filtered through a Celite column (0.5 cm × 2 cm) supported on glass wool. The blue filtrate (~3 mL) was layered with hexanes (~6 mL) and placed in the glove box freezer at -35 °C. The

solution was allowed to crystallize for ~3 days, after which a layer of pale blue, nearly colorless, crystals was observed. The colorless supernatant was decanted from the material and the crystals dried in vacuo for ~20 min to give a pale blue microcrystalline solid (88.7 mg, 68 %). Crystals suitable for X-ray analysis were grown at -35°C from a THF/hexane vapor diffusion. Anal. Calcd for $C_{30}H_{39}K_1O_6S_1Si_1$: C, 60.57; H, 6.61 Found: C, 60.52; H, 6.84. ^{1}H NMR (THF-d_8, 20 ºC, 400 MHz): δ 3.52 (s, 24 H, 18-crown-6), 7.03-7.10 (m, 9 H, meta and para CH), 7.75 (d, 6 H, J_{HH} = 5.7 Hz, ortho CH). ^{13}C{^{1}H} NMR (THF-d_8, 22 ºC, 100 MHz): δ 71.22 (18-crown-6), 126.76 (*para*-Ph), 126.94 (*meta*-Ph), 136.78 (*ortho*-Ph), 147.75 (*ipso*-Ph). ^{29}Si{^{1}H} NMR (THF-d_8, 21 ºC, 79.5 MHz): δ -7.35 (s, S*Si*). IR (KBr pellet, cm^{-1}): 3134(w), 3059(w), 3044(w sh), 3009(w), 2990(w), 2949(w sh), 2893(s), 2861(m sh), 2824(w), 2797(w), 2747(w), 2713(w), 2689(w), 1473(m), 1455(w), 1426(m), 1385(w sh), 1352(m), 1303(w sh), 1283(w), 1250(m), 1240(w sh), 1181(w), 1109(s), 1060(w sh), 1029 (w), 998(w), 963(s), 914(w), 873(w), 837(w), 743(w), 703(s), 689(m sh), 669(w), 624(w), 599(s), 530(w), 499(m), 459(w), 431(w), 421(w).

Synthesis of [K(18-crown-6)][Se-SiPh$_3$] (4). To a stirring, orange solution of [K(18-crown-6)][SiPh$_3$] (**1**) (117.0 mg, 0.21 mmol) in THF (2 mL) was added 1 equiv of selenium (17.2 mg, 0.22 mmol). An immediate color change to dark yellow was observed. Following stirring at ambient temperature for ~15 min, the solution was filtered through a Celite column (0.5 cm × 2 cm) supported on glass wool, layered with hexanes (~6 mL) and placed in the glove box freezer at -35 °C. Dark yellow crystals deposited from solution overnight. The crystals were isolated by decanting off the colorless supernatant. The crystals were immediately re-dissolved in THF (~2.5 mL) and allowed to stir at ambient temperature for ~15 min before the solution was filtered through a Celite column (0.5 cm × 2 cm) supported on glass wool. The dark yellow filtrate (~3 mL) was layered with hexanes (~6 mL) and placed in the glove box freezer at -35 °C. The

solution was allowed to crystallize for ~3 days, after which a layer of dark yellow crystals was observed. The colorless supernatant was decanted from the material and the crystals dried in vacuo for ~20 min to give a yellow-green microcrystalline solid (117.7 mg, 95 %). Crystals suitable for X-ray analysis were grown at -35 °C from a THF/hexane (1:3) layered solution. Anal. Calcd for $C_{30}H_{39}K_1O_6Se_1Si_1\cdot(OC_4H_8)$: C, 57.20; H, 6.64 Found: C, 57.37; H 6.67. ^{1}H NMR (THF-d_8, 21 ºC, 400 MHz): δ 3.52 (s, 24 H, 18-crown-6), 7.02-7.09 (m, 9 H, meta and para CH), 7.77 (d, 6 H, J_{HH} = 6.2 Hz, ortho CH). ^{13}C{^{1}H} NMR (THF-d_8, 21 ºC, 100 MHz): δ 71.08 (18-crown-6), 126.72 (*para*-Ph), 126.95 (*meta*-Ph), 137.07 (*ortho*-Ph), 146.87 (*ipso*-Ph). ^{29}Si{^{1}H} NMR (THF-d_8, 25 ºC, 79.5 MHz): δ -4.13 (s, Se*Si*). ^{77}Se{^{1}H} NMR (THF-d_8, 24 ºC, 76.3 MHz): δ -547.35 (s, *Se*Si). IR (KBr pellet, cm^{-1}): 3133(w), 3060(m), 3061(w), 3030(w), 2991(w), 2975(w sh), 2949(w sh), 2899(s), 2860(m sh), 2841(m), 2806(w sh), 2749(w), 2728(w), 2700(w), 1474(m), 1456(m), 1427(s), 1386(w sh), 1351(s), 1329(w), 1301(w sh), 1283(m), 1248(m), 1236(w sh), 1181(w), 1110(s), 1068(m sh), 1028(w), 1000(w), 962(s), 912(w), 864(w sh), 839(m), 807(w sh), 743(m), 702(s), 682(m), 668(w sh), 622(w), 536(s), 501(s), 452(w), 424(w).

Synthesis of [K(18-crown-6)][Te-SiPh$_3$] (5). To a stirring, orange solution of [K(18-crown-6)][SiPh$_3$] (**1**) (124.3 mg, 0.22 mmol) in THF (2 mL) was added 1 equiv of tellurium (29.1 mg, 0.23 mmol). A color change was observed within ~1 h from orange to red-pink. Following stirring at ambient temperature for ~1 h, the solution was filtered through a Celite column (0.5 cm × 2 cm) supported on glass wool, layered with hexanes (~6 mL) and placed in the glove box freezer at -35 °C. The solution was allowed to crystalllize overnight, affording the deposition of dark pink crystals. The crystals were isolated by decanting off the nearly colorless supernatant and were immediately re-dissolved in THF (~1.5 mL). The solution was allowed to stir at

ambient temperature for ~5 min before being filtered through a Celite column (0.5 cm × 2 cm) supported on glass wool. The pale red-pink filtrate (~1.5 mL) was layered with hexanes (~4 mL) and placed in the glove box freezer at -35 °C. The solution was allowed to crystallize for ~48 h, after which a layer of pale dark pink crystals was observed. The colorless supernatant was decanted from the material and the crystals dried in vacuo for ~15 min to give a dark pink microcrystalline solid (112.9 mg, 74 %). Crystals suitable for X-ray analysis were grown at -35 °C from a THF/hexane (1:3) layered solution. Anal. Calcd for $C_{30}H_{39}K_1O_6Te_1Si_1 \cdot (OC_4H_8)$: C, 53.56; H, 6.21 Found: C, 53.61; H 6.14. ^{1}H NMR (THF-d_8, 24 ºC, 400 MHz): δ 3.52 (s, 24 H, 18-crown-6), 7.01-7.09 (m, 9 H, meta and para CH), 7.78 (d, 6 H, J_{HH} = 6.3 Hz, ortho CH). ^{13}C{^{1}H} NMR (THF-d_8, 25 ºC, 100.6 MHz): δ 71.08 (18-crown-6), 126.63 (*para*-Ph), 126.95 (*meta*-Ph), 137.46 (*ortho*-Ph), 145.65(*ipso*-Ph). ^{29}Si{^{1}H} NMR (THF-d_8, 19 ºC, 79.5 MHz): δ -11.67 (s, Te*Si*). ^{125}Te{^{1}H} NMR (THF-d_8, 24 ºC, 126.1 MHz): δ -1303.40 (s, *Te*Si). IR (KBr pellet, cm^{-1}): 3131(w), 3061(m), 3059(m), 3030(w), 2991(w sh), 2975(m sh), 2947(m sh), 2896(s), 2861(s sh), 2841(m), 2805(w sh), 2746(w), 2714(w), 2704(w), 1975(w), 1473(m), 1465(m), 1427(s), 1351(s), 1301(w sh), 1284(m), 1248(m), 1239(m sh), 1185(m), 1114(s), 1078(m sh), 1045(m), 1017(w), 962(s), 917(m), 885(w sh), 837(m), 819(w sh), 742(m), 702(s), 690(m), 672(w sh), 622(w), 530(w sh), 508(s), 512(s sh), 440(w), 425(w).

Synthesis of [K(18-crown-6)][S-SiPh$_2$^{t}Bu] (6). To a stirring, orange solution of [K(18-corwn-6)][SiPh$_2$^{t}Bu] (**2**) (92.8 mg, 0.17 mmol) in THF (2 mL) was added 0.125 equiv of S_8 (5.8 mg, 0.023 mmol). An immediate color change to blue was observed. Following stirring at ambient temperature for ~10 min, the solution was filtered through a Celite column (0.5 cm × 2 cm) supported on glass wool, layered with hexanes (~6 mL) and placed in the glove box freezer at -35 °C. Pale blue, almost colorless, crystals deposited from solution overnight. The crystals were

isolated by decanting off the colorless supernatant. The crystals were immediately re-dissolved in THF (~2.5 mL) and allowed to stir at ambient temperature for ~15 min before the solution was filtered through a Celite column (0.5 cm × 2 cm) supported on glass wool. The blue filtrate (~2 mL) was layered with hexanes (~5 mL) and placed in the glove box freezer at -35 °C. The solution was allowed to crystallize overnight, after which a layer of pale blue, nearly colorless, crystals was observed. The colorless supernatant was decanted from the material and the crystals dried in vacuo to give a pale blue microcrystalline solid (60.6 mg, 62 %). Crystals suitable for X-ray analysis were grown at -35 °C from a THF/Et_2O (1:4) layered solution. Anal. Calcd for $C_{28}H_{43}K_1O_6S_1Si_1 \cdot (OC_4H_8)$: C, 59.40; H, 7.94 Found: C, 59.30; H, 7.84. ^{1}H NMR (THF-d_8, 27 ºC, 400 MHz): δ 0.98 (s, 9 H, Me), 3.52 (s, 24 H, 18-crown-6), 7.02-7.13 (m, 9 H, meta and para CH), 8.07 (d, 6 H, J_{HH} = 6.5 Hz, ortho CH). ^{13}C{^{1}H} NMR (THF-d_8, 27 ºC, 100 MHz): δ 21.46 ($C(CH_3)_3$), 29.40 ($C(CH_3)_3$), 71.11 (18-crown-6), 126.40 (*para*-Ph), 126.65 (*meta*-Ph), 137.49 (*ortho*-Ph), 146.66 (*ipso*-Ph). ^{29}Si{^{1}H} NMR (THF-d_8, 23 ºC, 79.5 MHz): δ 2.58 (s, S*Si*). IR (KBr pellet, cm^{-1}): 3062(w), 3043(w), 2996(w), 2988(w sh), 2955(m), 2935(m sh), 2889(m), 2858(m sh), 2842(m sh), 2800(w sh), 2748(w), 2715(w), 2692(w), 1981(w), 1473(w), 1457(w), 1426(w), 1381(w), 1352(s), 1302(w sh), 1285(w), 1251(w), 1238(w sh), 1183(w), 1112(s), 1061(w sh), 1030(w sh), 1008(w), 1000(w sh), 963(s), 916(w), 840(w), 818(w), 747(w), 738(w), 705(m), 686(w), 660(w), 630(w), 615(w), 570(w), 532(w), 492(w).

Synthesis of [K(18-crown-6)][Se-SiPh$_2$^{t}Bu] (7). To a stirring, orange solution of [K(18-crown-6)][SiPh$_2$^{t}Bu] (**2**) (79.6 mg, 0.15 mmol) in THF (3 mL) was added 1 equiv of selenium (13.0 mg, 0.16 mmol). An immediate color change to dark yellow-green was observed upon. Following stirring at ambient temperature for ~15 min, the solution was filtered through a Celite column (0.5 cm × 2 cm) supported on glass wool, layered with hexanes (~6 mL) and placed in the glove

box freezer at -35 °C. Dark yellow-green crystals deposited from solution overnight. The crystals were isolated by decanting off the pale yellow supernatant. The crystals were immediately re-dissolved in THF (~2.5 mL) and allowed to stir at ambient temperature for ~15 min before the solution was filtered through a Celite column (0.5 cm × 2 cm) supported on glass wool. The dark yellow-green filtrate (~3 mL) was layered with hexanes (~6 mL) and placed in the glove box freezer at -35 °C. The solution was allowed to crystallize overnight, after which a layer of dark yellow-green crystals was observed. The colorless supernatant was decanted from the material and the crystals dried in vacuo for ~20 min to give a light brown microcrystalline solid (77.6 mg, 85 %). Crystals suitable for X-ray analysis were grown at -35 °C from a THF/hexane vapor diffusion. Anal. Calcd for $C_{28}H_{43}K_1O_6Se_1Si_1$: C, 54.09; H, 6.97 Found: C, 54.24; H 6.83. ^{1}H NMR (THF-d_8, 22 ºC, 400 MHz): δ 1.01 (s, 9 H, Me), 3.52 (s, 24 H, 18-crown-6), 7.01-7.12 (m, 9 H, meta and para CH), 8.10 (d, 6 H, J_{HH} = 7.2 Hz, ortho CH). ^{13}C{^{1}H} NMR (THF-d_8, 22 ºC, 100 MHz): δ 20.99 (*C*(CH_3)$_3$), 29.56 (C(*C*H_3)$_3$), 70.98 (18-crown-6), 126.33 (*para*-Ph), 126.68 (*meta*-Ph), 137.88 (*ortho*-Ph), 145.74 (*ipso*-Ph). ^{29}Si{^{1}H} NMR (THF-d_8, 20 ºC, 79.5 MHz): δ 10.05 (s, Se*Si*). ^{77}Se{^{1}H} NMR (THF-d_8, 26 ºC, 76.3 MHz): δ -580.75 (s, *Se*Si). IR (KBr pellet, cm^{-1}): 3062(w), 3045(w), 3000(w sh), 2989(w sh), 2957(m), 2935(m sh), 2884(s), 2860(s), 2798(w sh), 2747(w), 2716(w), 2693(w), 1473(m), 1456(w), 1426(w), 1382(w), 1352(s), 1286(w), 1250(m), 1241(w sh), 1180(w), 1152(w sh), 1132(w sh), 1111(s), 1061(m sh), 1045(w sh), 1031(w sh), 1008(w), 997(w), 962(s), 916(w), 839(w), 816(w), 747(w), 740(w), 704(m), 692(w sh), 683(w sh), 669(w), 623(w), 597(w), 528(m), 486(m), 441(w).

Synthesis of [K(18-crown-6)][Te-SiPh$_2$^{t}Bu] (8). To a stirring, orange solution of [K(18-crown-6)][SiPh$_2$^{t}Bu] (**2**) (101.3 mg, 0.19 mmol) in THF (2 mL) was added 1 equiv of tellurium (24.1 mg, 0.19 mmol). A color change was observed within ~1 h from orange to pale purple.

Following stirring at ambient temperature for ~1 h, the solution was filtered through a Celite column (0.5 cm × 2 cm) supported on glass wool, layered with hexanes (~5 mL) and placed in the glove box freezer at -35 °C. The solution was allowed to crystalllize for ~4 days, affording the deposition of pale purple, almost colorless, crystals. The crystals were isolated by decanting off the nearly colorless supernatant and were immediately re-dissolved in THF (~1.5 mL). The solution was allowed to stir at ambient temperature for ~5 min before being filtered through a Celite column (0.5 cm × 2 cm) supported on glass wool. The pale purple filtrate (~1.5 mL) was layered with hexanes (~3 mL) and placed in the glove box freezer at -35 °C. The solution was allowed to crystallize overnight, after which a layer of pale purple crystals was observed. The colorless supernatant was decanted from the material and the crystals dried in vacuo for ~20 min to give a pale purple microcrystalline solid (100.1 mg, 81 %). Crystals suitable for X-ray analysis were grown at -35 °C from a THF/hexane (1:3) layered solution. Anal. Calcd for $C_{28}H_{43}K_1O_6Te_1Si_1 \cdot 0.5(OC_4H_8)$: C, 51.00; H, 6.71 Found: C, 51.08; H 6.66. ^{1}H NMR (THF-d_8, 23 ºC, 400 MHz): δ 1.05 (s, 9 H, Me), 3.53 (s, 24 H, 18-crown-6), 7.02-7.09 (m, 9 H, meta and para CH), 8.09 (d, 6 H, J_{HH} = 7.2 Hz, ortho CH). ^{13}C{^{1}H} NMR (THF-d_8, 23 ºC, 100 MHz): δ 20.04 (*C*$(CH_3)_3$), 29.80 (C(*C*$H_3)_3$), 71.06 (18-crown-6), 126.26 (*para*-Ph), 126.72 (*meta*-Ph), 138.41 (*ortho*-Ph), 144.78 (*ipso*-Ph). ^{29}Si{^{1}H} NMR (THF-d_8, 19 ºC, 79.5 MHz): δ 5.52 (s, Te*Si*). ^{125}Te{^{1}H} NMR (THF-d_8, 24 ºC, 126.1 MHz): δ -1360.10 (s, *Te*Si). IR (KBr pellet, cm^{-1}): 3163(w), 3126(w), 3061(m), 3040(m), 3013(w), 2952(s sh), 2896(s), 2849(s), 2827(w sh), 2798(w sh), 2746(w), 2711(w), 2691(w), 1979(w), 1561(w), 1471(s), 1454(m), 1426(m), 1382(w), 1352(s), 1285(m), 1249(s), 1239(m sh), 1185(w), 1150(w sh), 1110(s), 1069(w sh), 1058(w sh), 1030(w), 1008(w), 997(w), 963(s), 936(w sh), 916(w), 873(w), 839(s), 817(m),

795(w), 745(m), 741(m), 702(s), 692(m), 680(m), 623(w), 607(w sh), 591(m), 530(w), 505(s), 479(m), 436(w).

X-ray Crystallography. Data for **2**, **3**·0.5THF, **4**·THF, **5**·THF, **6**·0.5THF, **7**·0.5THF and **8**·0.5THF were collected on a Bruker AXS SMART APEX II charge coupled-device (CCD) diffractometer, equipped with graphite monochromatized MoKα X-ray source (α = 0.7107 Å). Crystals were mounted in a nylon cryoloop using Paratone-N oil under argon gas and all data were collected at a temperature of 120(1) K with a Cryo Industries of America Cryocool G2 cooling device. A hemisphere of data was collected using ω scans with 0.3º frame widths. Data collection and cell parameter determination were conducted using SMART software (version 5.632, **2005**, Bruker AXS, Inc., Madison, Wisconsin 53719). Integration of data frames, including Lorentz-polarization corrections, and final cell parameter refinement were performed using SAINT^{+} software (version 6.45, **2003**, Bruker AXS, Inc., Madison, Wisconsin 53719). The data were corrected for absorption using the SADABS program (version 2.05, **2002**, George Sheldrick, University of Göttingen, Germany). Decay of reflection intensity was monitored via analysis of redundant frames. The structure was solved using direct methods and difference Fourier techniques. All hydrogen atom positions were idealized and rode on the atom they were attached to. Structure solution, refinement, graphics, and creation of publication materials were performed using SHELXTL (version 6.10, **2001**, Bruker AXS, Inc., Madison, Wisconsin 53719). The program PLATON-SQUEEZE was used to remove disordered solvent molecules from the unit cell where appropriate and details are in the crystallographic files.[49] A summary of relevant crystallographic data for all the compounds are presented in Table 4.

Acknowledgements. We thank the U.S. Department of Energy, Office of Science, Basic Energy Sciences, Early Career Program (research activities) and the Heavy Element Chemistry Program

(manuscript preparation) under contract DE-AC52-06NA25396. J. L. B. thanks the G. T. Seaborg Institute at Los Alamos National Laboratory for a Postdoctoral Fellowship.

Supporting Information Available: Crystallographic details for **2-8** and spectroscopic data for **1**-**8**. This material is available free of charge via the Internet at http://pubs.acs.org.

References

(1) Kuckmann, T. I.; Hermsen, M.; Bolte, M.; Wagner, M.; Lerner, H.-W. *Inorg. Chem.* **2005**, *44*, 3449.

(2) Kuckmann, T. I.; Schodel, F.; Sanger, I.; Bolte, M.; Wagner, M.; Lerner, H.-W. *Organometallics* **2008**, *27*, 3272.

(3) Kuckmann, T.; Schodel, F.; Sanger, I.; Bolte, M.; Wagner, M.; Lerner, H.-W. *Eur. J. Inorg. Chem.* **2010**, 468.

(4) Gerlach, C. P.; Arnold, J. *Inorg. Chem.* **1996**, *35*, 5770.

(5) Komuro, T.; Kawaguchi, H.; Tatsumi, K. *Inorg. Chem.* **2002**, *41*, 5083.

(6) Sydora, O. L.; Wolczanski, P. T.; Lobkovsky, E. B.; Rumberger, E.; Hendrickson, D. N. *Chem. Commun.* **2004**, 650.

(7) Yu, S.-B. *Polyhedron* **1992**, *11*, 2115.

(8) Medina, I.; Jacobsen, H.; Mague, J. T.; Fink, M. J. *Inorg. Chem.* **2006**, *45*, 8844.

(9) Deng, L.; Majumbar, A.; Lo, W.; Holm, R. H. *Inorg. Chem.* **2010**, *49*, 11118.

(10) Preuss, F.; Niochl, H.; Kaub, J. *Z. Naturforsch., B: Chem. Sci.* **1986**, *41*, 1085.

(11) Komuro, T.; Matsuo, T.; Kawaguchi, H.; Tatsumi, K. *Dalton Trans.* **2004**, 1618.

(12) Komuro, T.; Kawaguchi, H.; Tatsumi, K. *Inorg. Chem.* **2002**, *41*, 5083.

(13) Khadka, C. B.; MacDonald, D. G.; Lan, Y.; Powell, A. K.; Fenske, D.; Corrigan, J. F. *Inorg. Chem.* **2010**, *49*, 7289.

(14) DeGroot, M. W.; Corrigan, J. F. *Angew. Chem.* **2004**, *116*, 5469.

(15) DeGroot, M. W.; C, K.; Rosner, H.; Corrigan, J. F. *J. Cluster Sci.* **2006**, *17*, 97.

(16) Khadka, C. B.; Eichhofer, A.; Weigend, F.; Corrigan, J. F. *Inorg. Chem.* **2012**, *51*, 2747.

(17) Tuna, F.; Smith, C. A.; Bodensteiner, M.; Ungur, L.; Chibotaru, L. F.; McInnes, E. J. L.; Winpenny, R. E. P.; Collison, D.; Layfield, R. A. *Angew. Chem. Int. Ed.* **2012**, *51*, 6976.

(18) Chadwick, S.; Englich, U.; Ruhlandt-Senge, K. *Organometallics* **1997**, *16*, 5792.

(19) Gindelberger, D. E.; Arnold, J. *Organometallics* **1994**, *13*, 4462.

(20) Bonasia, P. J.; Christou, V.; Arnold, J. *J. Am. Chem. Soc.* **1993**, *115*, 6777.

(21) Gindelberger, D. E.; Arnold, J. *Inorg. Chem.* **1994**, *33*, 6293.

(22) Gaunt, A. J.; Reilly, S. D.; Enriquez, A. E.; Scott, B. L.; Ibers, J. A.; Sekar, P. *Inorg. Chem.* **2008**, *47*, 29.

(23) Jones, M. B.; Gaunt, A. J.; Gordon, J. C.; Kaltsoyannis, N.; Neu, M. P.; Scott, B. L. *Chem. Sci.* **2013**, *4*, 1189.

(24) Macor, J. A.; Brown, J. L.; Cross, J. N.; Daly, S. R.; Gaunt, A. J.; Girolami, G. S.; Janicke, M. T.; Kozimor, S. A.; Neu, M. P.; Olson, A. C.; Reilly, S. D.; Scott, B. L. *Dalton Trans.* **2015**, *44*, 18923.
(25) H.-W, L. *Coord. Chem. Rev.* **2005**, *249*, 781.
(26) Leich, V.; Lamberts, K.; Spaniot, T. P.; Okuda, J. *Dalton Trans.* **2014**, *43*, 14315.
(27) Benkeser, R. A.; Severson, R. G. *J. Am. Chem. Soc.* **1951**, *73*, 1424.
(28) Gilman, H.; Dunn, G. E. *J. Am. Chem. Soc.* **1951**, *73*, 5077.
(29) Gilman, H.; Wu, T. C. *J. Am. Chem. Soc.* **1951**, *73*, 4031.
(30) Gilman, H.; Peterson, D. J.; Wittenberg, D. *Chem. Ind.* **1958**, 1479.
(31) Gilman, H.; Lichtenwalter, G. D. *J. Am. Chem. Soc.* **1958**, *80*, 608.
(32) Reiter, B.; Hassler, K. *J. Organomet. chem.* **1994**, *467*, 21.
(33) Feher, F.; Plichta, P.; Guillery, R. *Tetraherdon lett.* **1970**, 4443.
(34) Feher, F.; Plichta, P.; Guillery, R. *Tetraherdon lett.* **1970**, 2889.
(35) Sakurai, H.; Okada, A.; Kira, M.; Yonezawa, K. *Tetraherdon lett.* **1971**, 1511.
(36) Sakurai, H.; Kondo, F. *J. Organomet. Chem.* **1975**, *92*, C46.
(37) Buncel, E.; Venkatachalam, T. K.; Edlund, U. *J. Organomet. Chem.* **1992**, *437*, 85.
(38) Corriu, R. J. P.; Guerin, C. *J. Chem. Soc., Chem. Commun.* **1980**, 168.
(39) Brefort, J. L.; Corriu, R.; Guerin, C.; Henner, B. *J. Organomet. Chem.* **1989**, *370*, 9.
(40) Weiss, E.; Hencken, G.; Kuehr, H. *Chem. Ber.* **1970**, *103*, 2868.
(41) Kleeberg, C.; Borner, C. *Eur. J. Inorg. Chem.* **2013**, 2799.
(42) Suginome, M.; Matsuda, T.; Ito, Y. *Organometallics* **2000**, *19*, 4647.
(43) Lerner, H.-W.; Scholz, S.; Bolte, M.; Wagner, M. *Z. Anorg. Allg. Chem.* **2004**, *630*, 443.
(44) Campion, B. K.; Heyn, R. H.; Tilley, T. D. *Organometallics* **1993**, *12*, 2584.
(45) Dias, H. V. R.; Olmstead, M. M.; Ruhlandt-Senge, K.; Power, P. P. *J. Organomet. Chem.* **1993**, *462*, 1.
(46) Komuro, T.; T, M.; Kawaguchi, H.; Tatsumi, K. *Dalton Trans.* **2004**, 1618.
(47) Kleeberg, C. *Dalton Trans.* **2013**, *42*, 8276.
(48) Monakhov, K. Y.; Zessin, T.; Linti, G. *Eur. J. Inorg. Chem.* **2010**, 322.
(49) Spek, A. L. *J. Appl. Crystallogr.* **2003**, *36*, 7.
(50) Klink, R.; Schrenk, C.; Schnepf, A. *Dalton Trans.* **2014**, *43*, 16097.
(51) Meihaus, K. R.; Long, J. R. *J. Am. Chem. Soc.* **2013**, *135*, 17952.
(52) Rodger, C.; Sheppard, N.; McFarlane, C.; McFarlane, W. *NMR and The Periodic Table. Ch.12: Group VI- Oxygen, Sulphur, Selenium, Tellurium*; Academic press Inc.: London, 1978.

Supporting Information For:

Synthesis and Characterization of

Potassium Aryl- and Alkyl-Substituted Silylchalcogenolate Ligands

Jessie L. Brown,[a] Michael T. Janicke,[a] Brian L. Scott[b] and Andrew J. Gaunt[*,a]

[a]Chemistry Division and [b]Materials Physics and Applications Division, Los Alamos National Laboratory, Los Alamos, New Mexico 87545, USA

*To whom correspondence should be addressed. Email: gaunt@lanl.gov

IR Spectra.

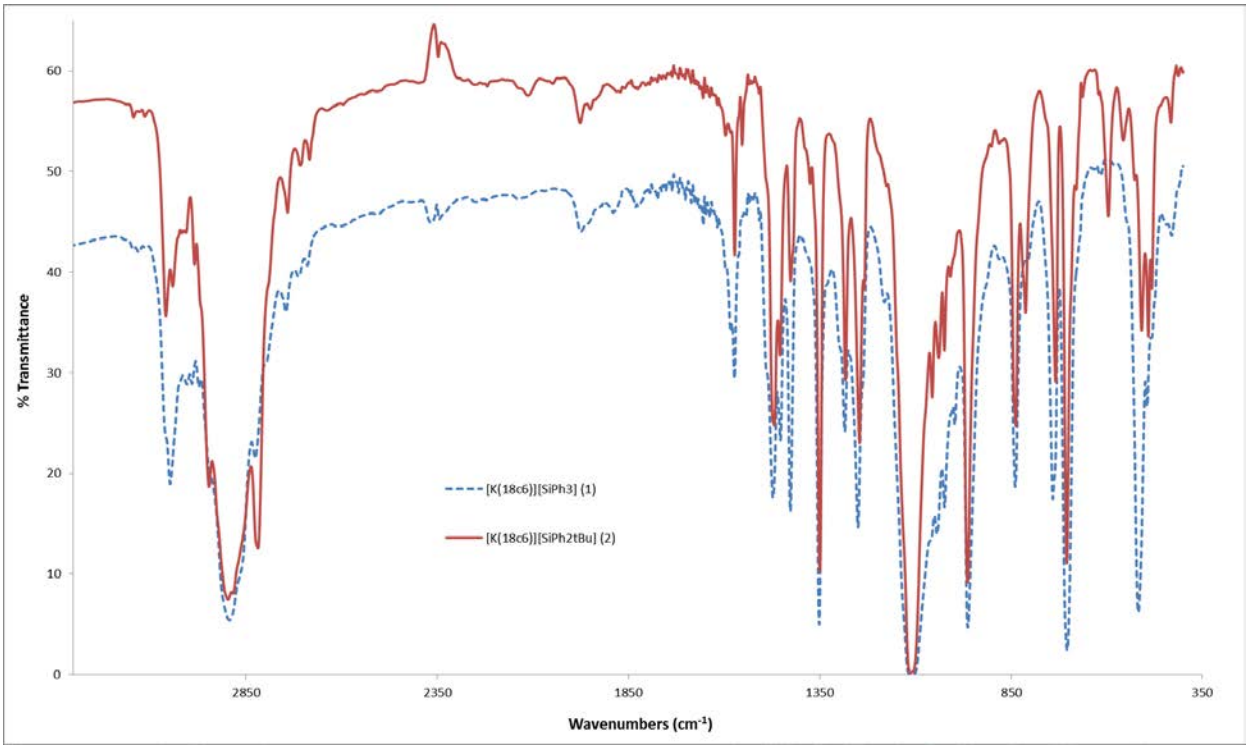

Figure S1. Overlay of IR spectra of **1** and **2** (KBr mull). The stretches observed from ~2400-2300 cm^{-1} are persistent artifacts from the instrument that were not able to be subtracted from the background.

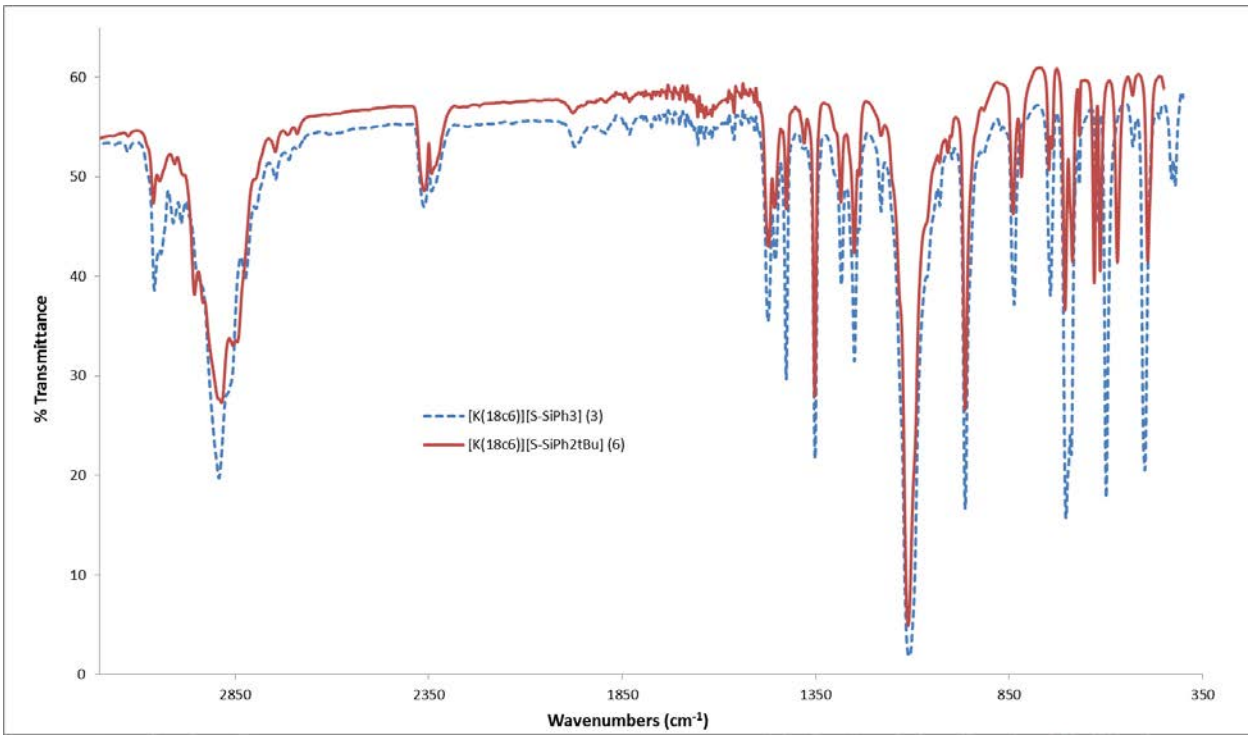

Figure S2. Overlay of IR spectra of **3** and **6** (KBr mull). The stretches observed from ~2400-2300 cm^{-1} are persistent artifacts from the instrument that were not able to be subtracted from the background.

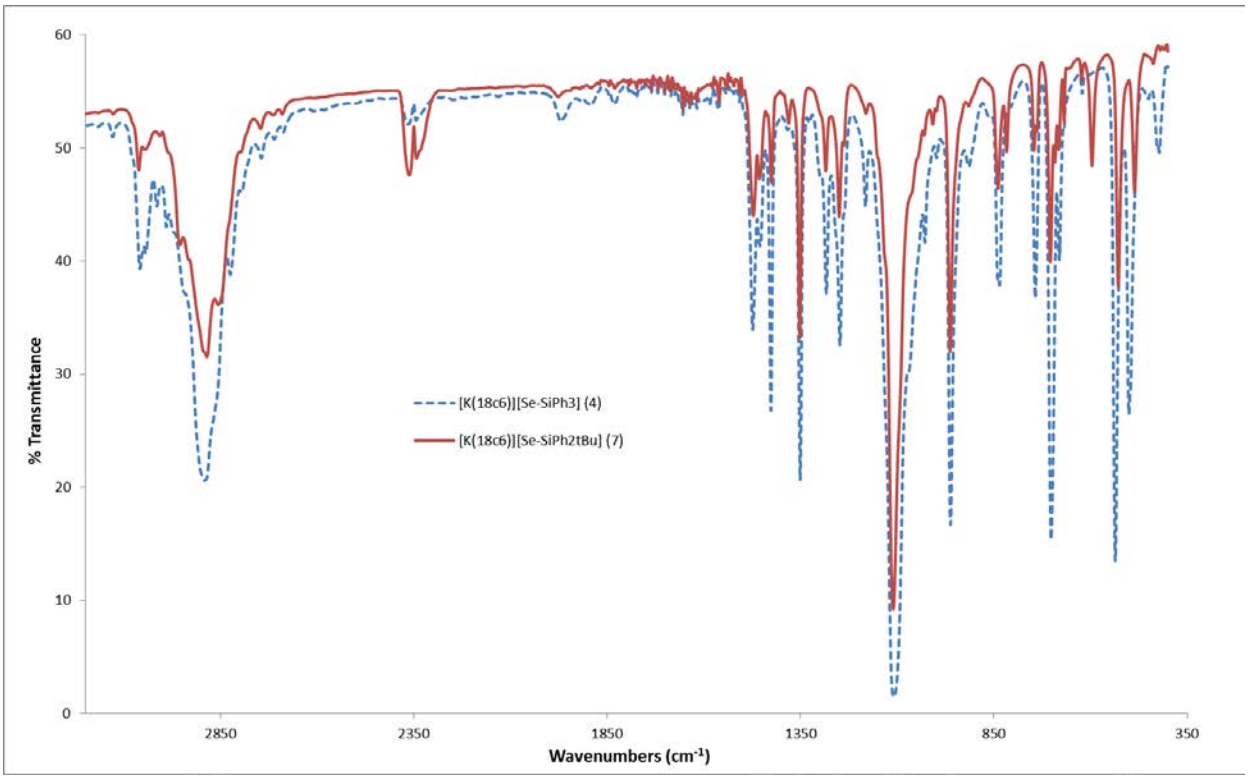

Figure S3. Overlay of IR spectra of **4** and **7** (KBr mull). The stretches observed from ~2400-2300 cm^{-1} are persistent artifacts from the instrument that were not able to be subtracted from the background.

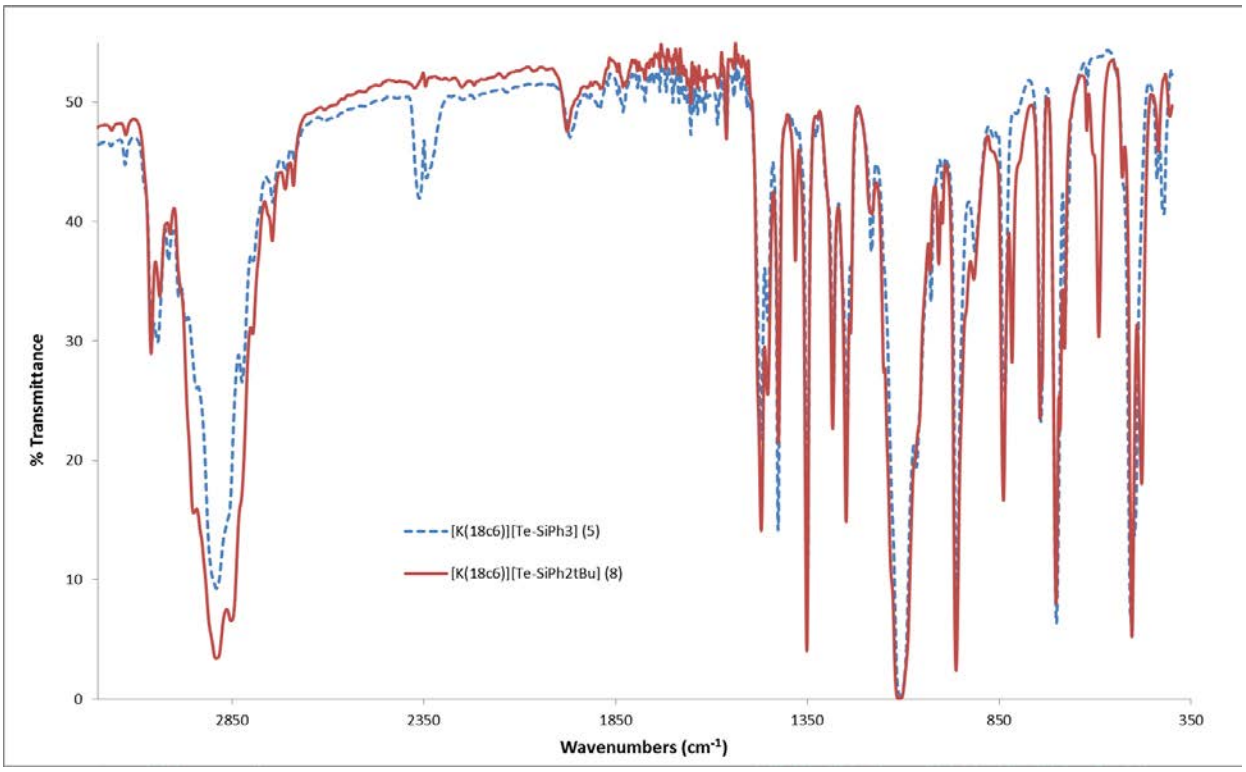

Figure S4. Overlay of IR spectra of **5** and **8** (KBr mull). The stretches observed from ~2400-2300 cm^{-1} are persistent artifacts from the instrument that were not able to be subtracted from the background.

NMR Spectra.

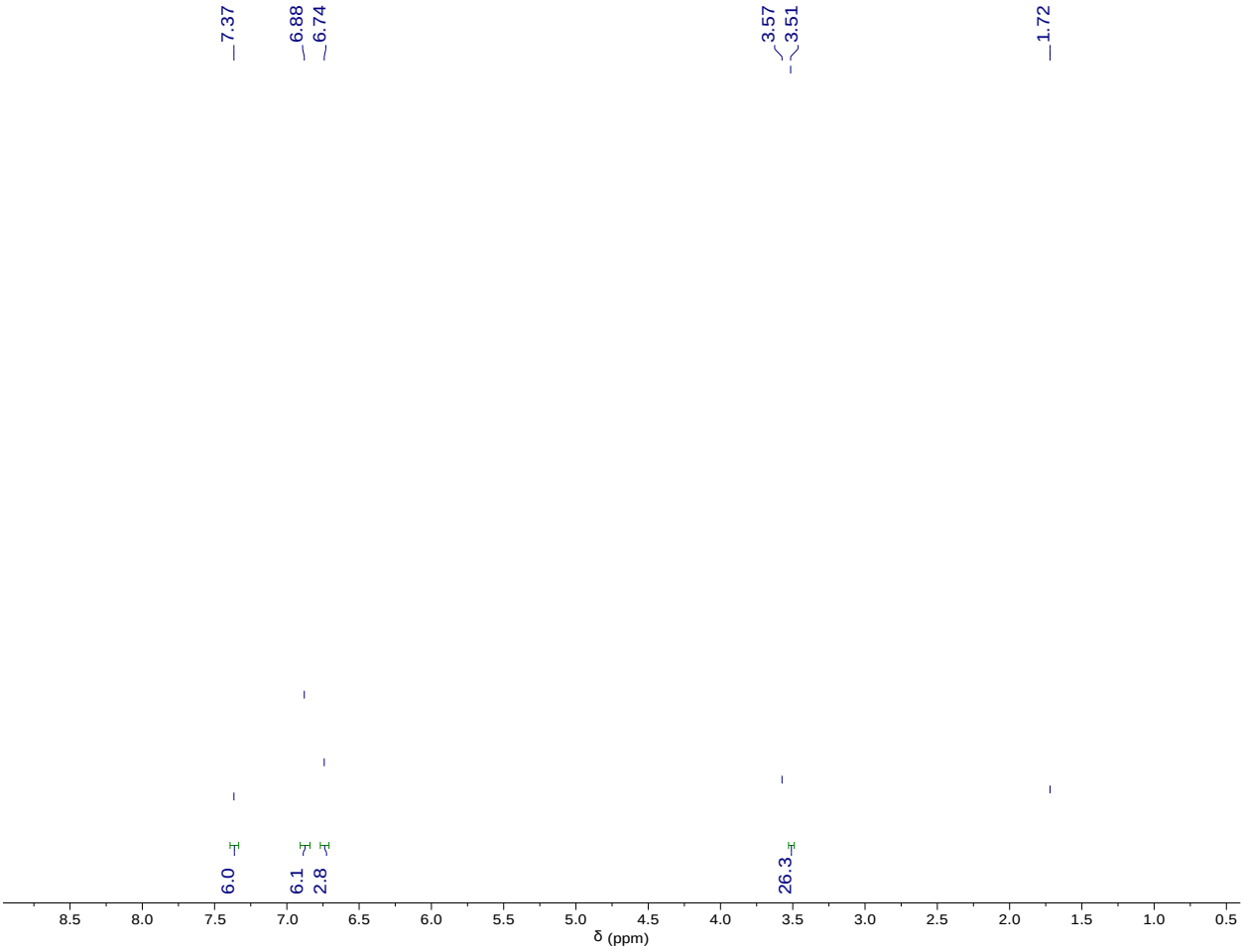

Figure S5. ^{1}H NMR spectrum of **1** in THF-d_8.

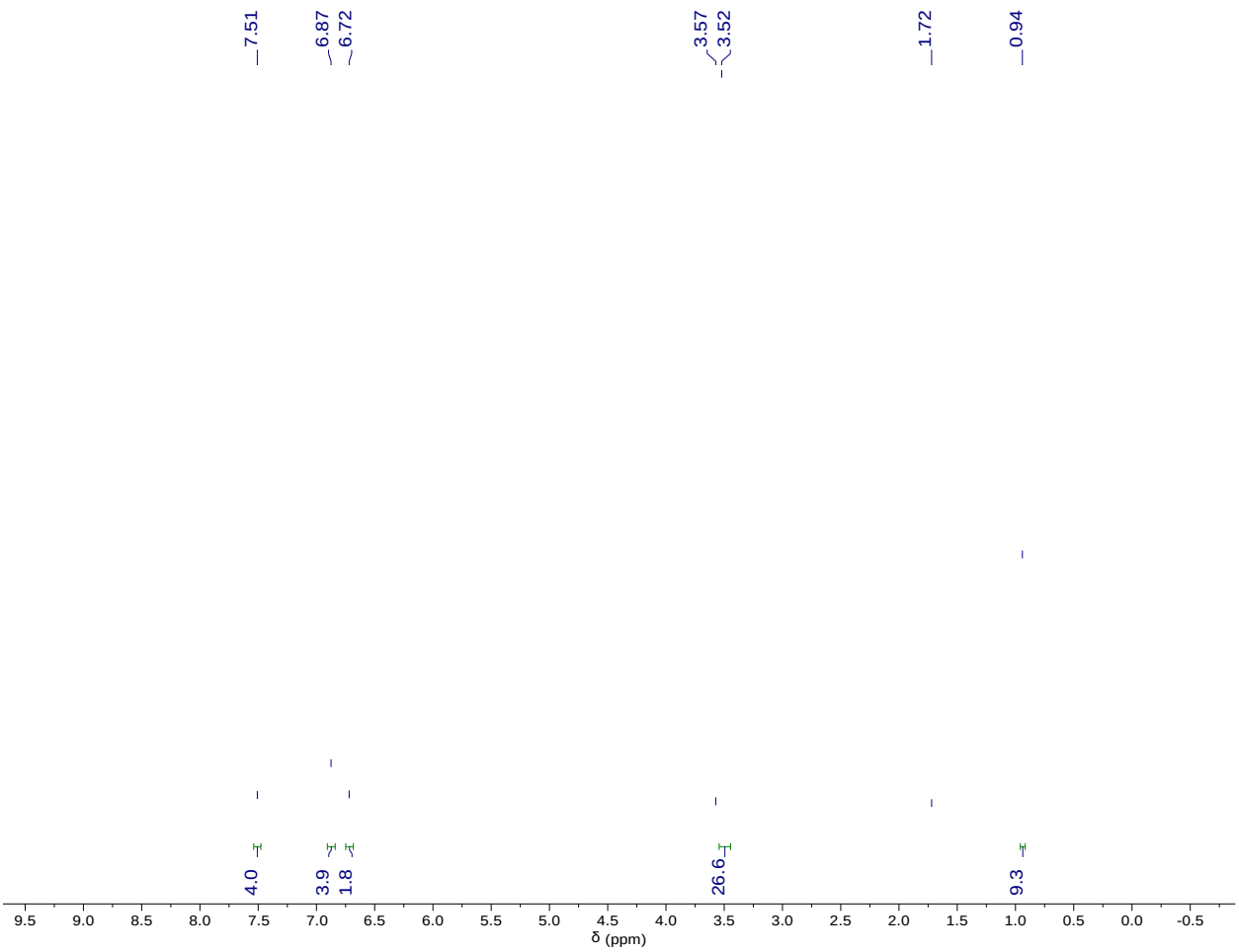

Figure S6. ^{1}H NMR spectrum of **2** in THF-d_8.

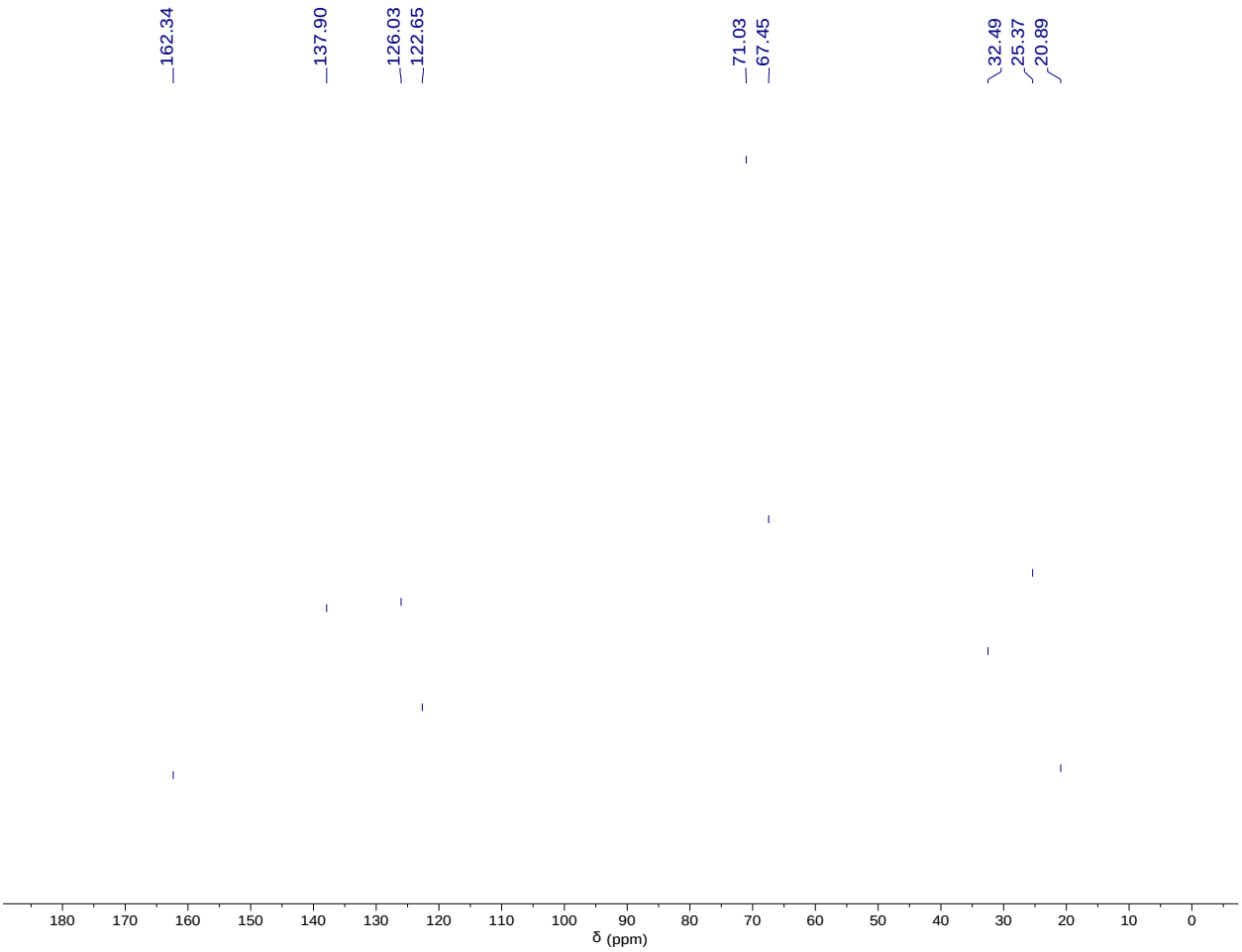

Figure S7. ^{13}C NMR spectrum of **2** in THF-d_8.

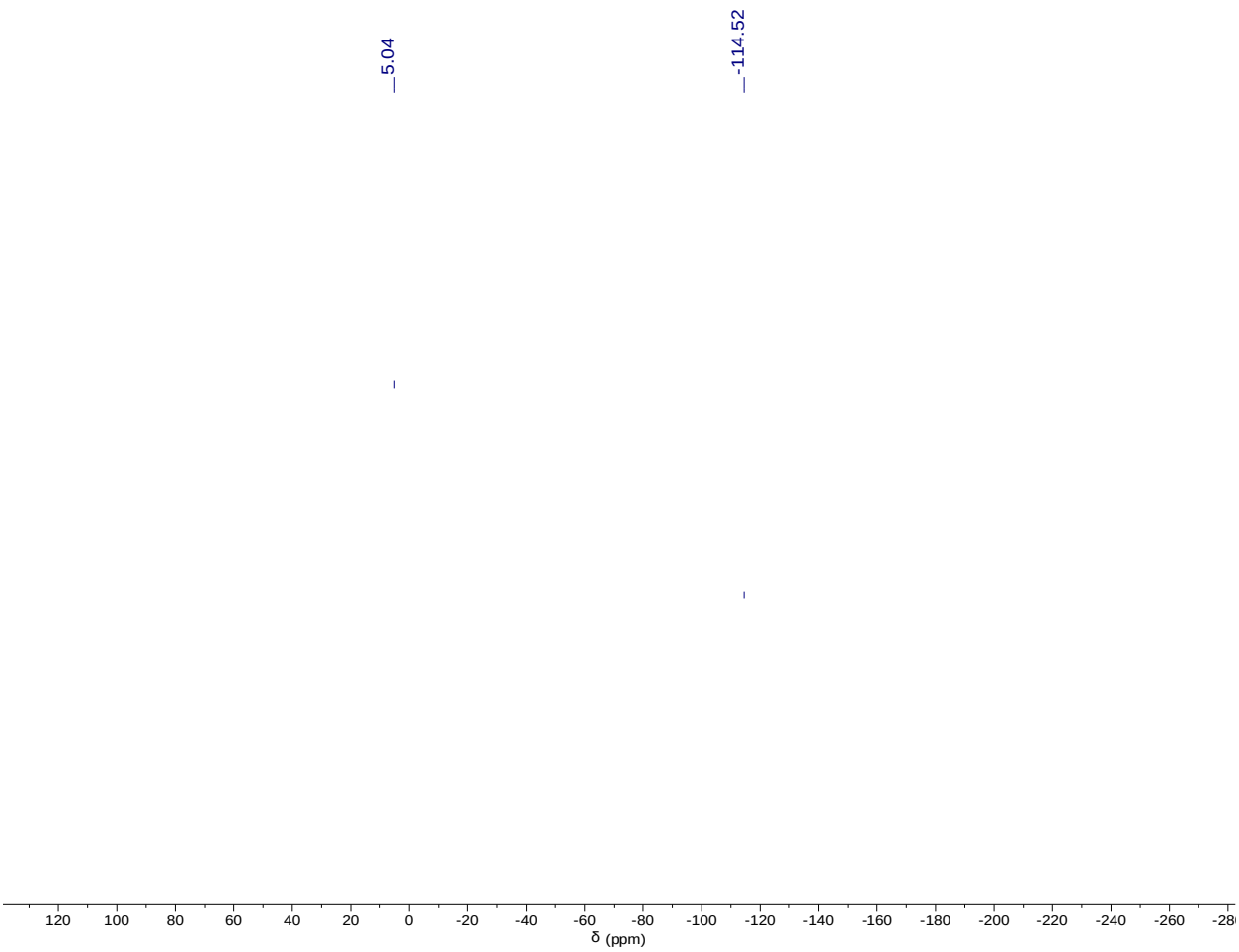

Figure S8. ^{29}Si NMR spectrum of **2** in THF-d_8. The resonance at -114.52 ppm is assignable to the borosilicate glass from the NMR tube.

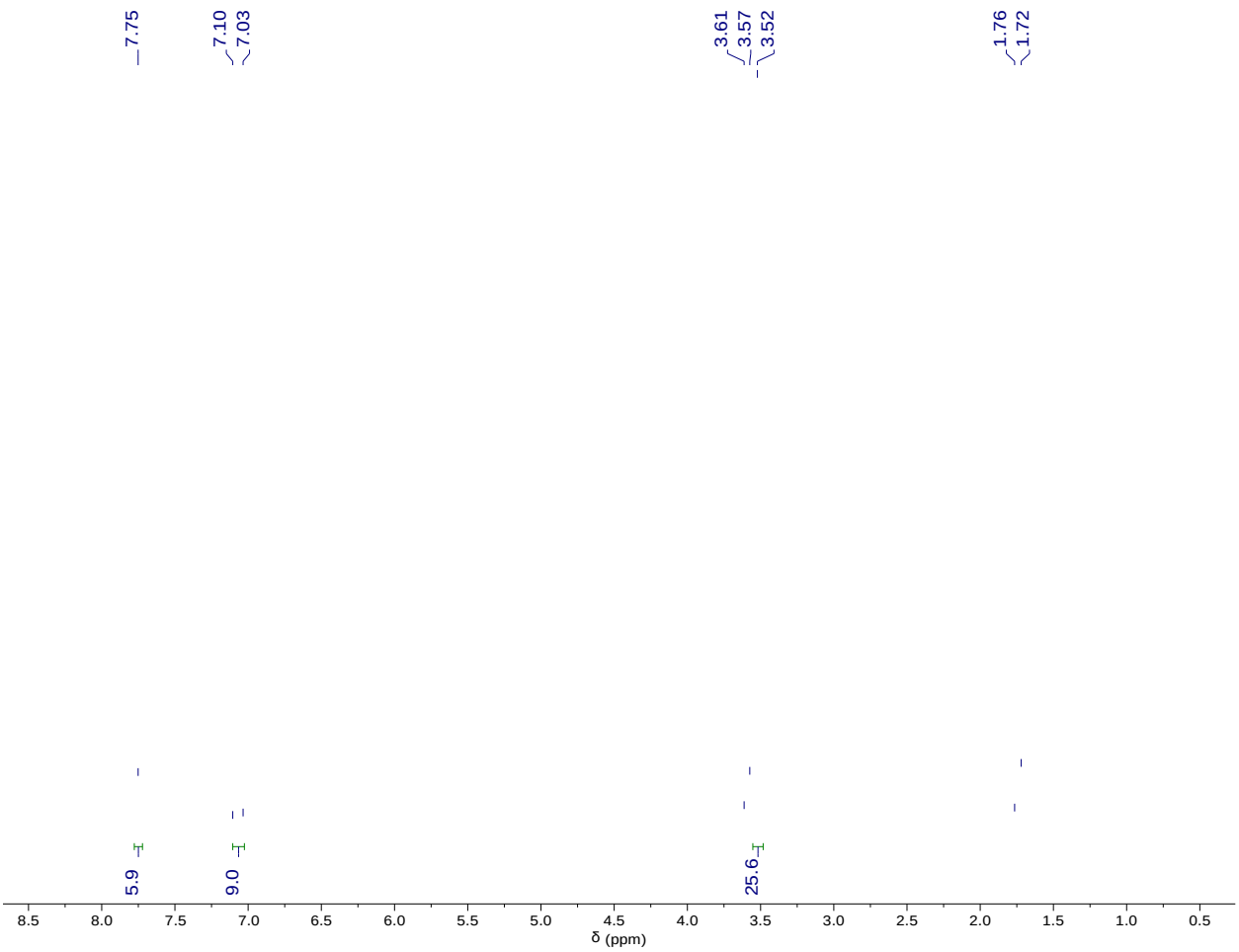

Figure S9. ^{1}H NMR spectrum of **3** in THF-d_8.

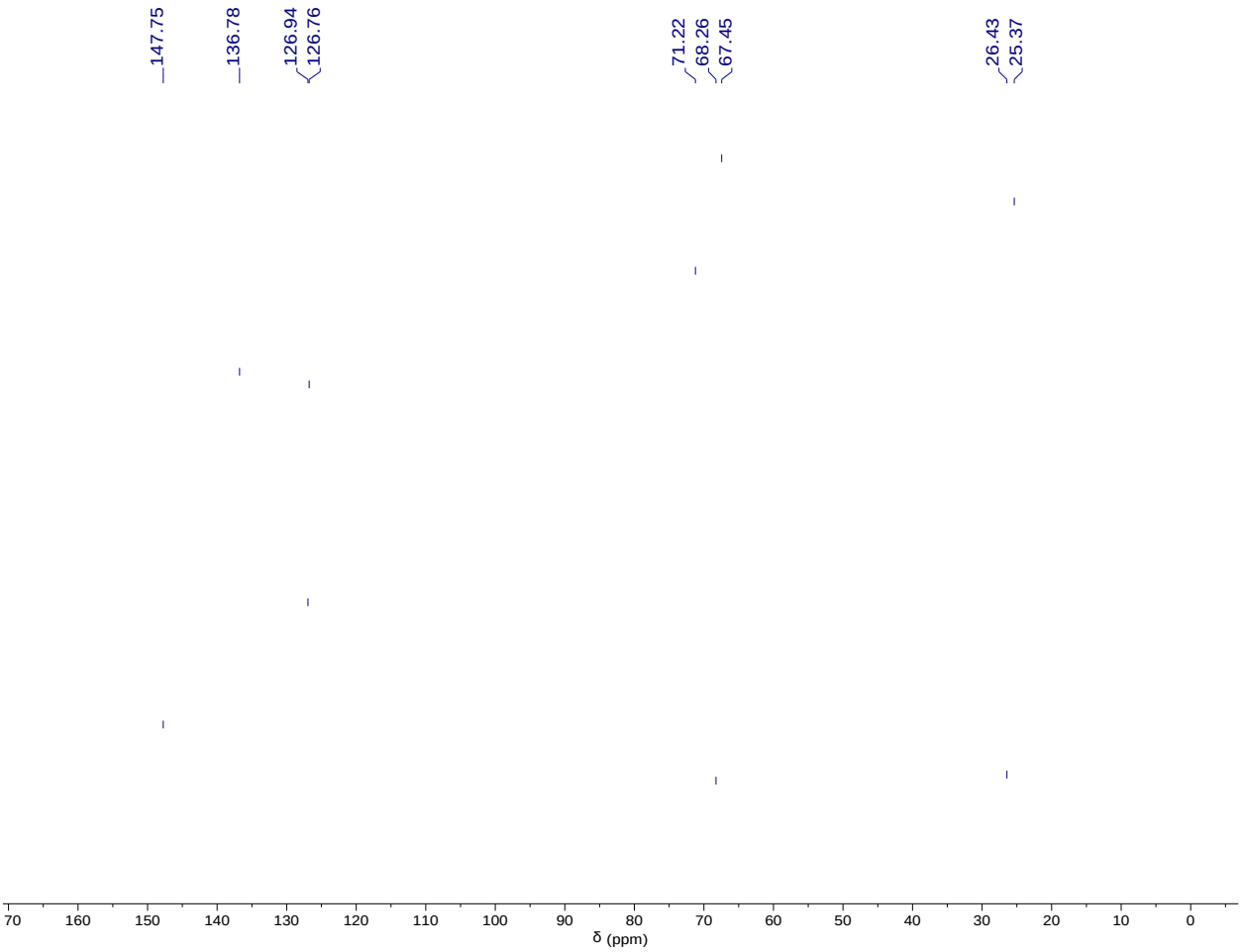

Figure S10. ^{13}C NMR spectrum of **3** in THF-d_8.

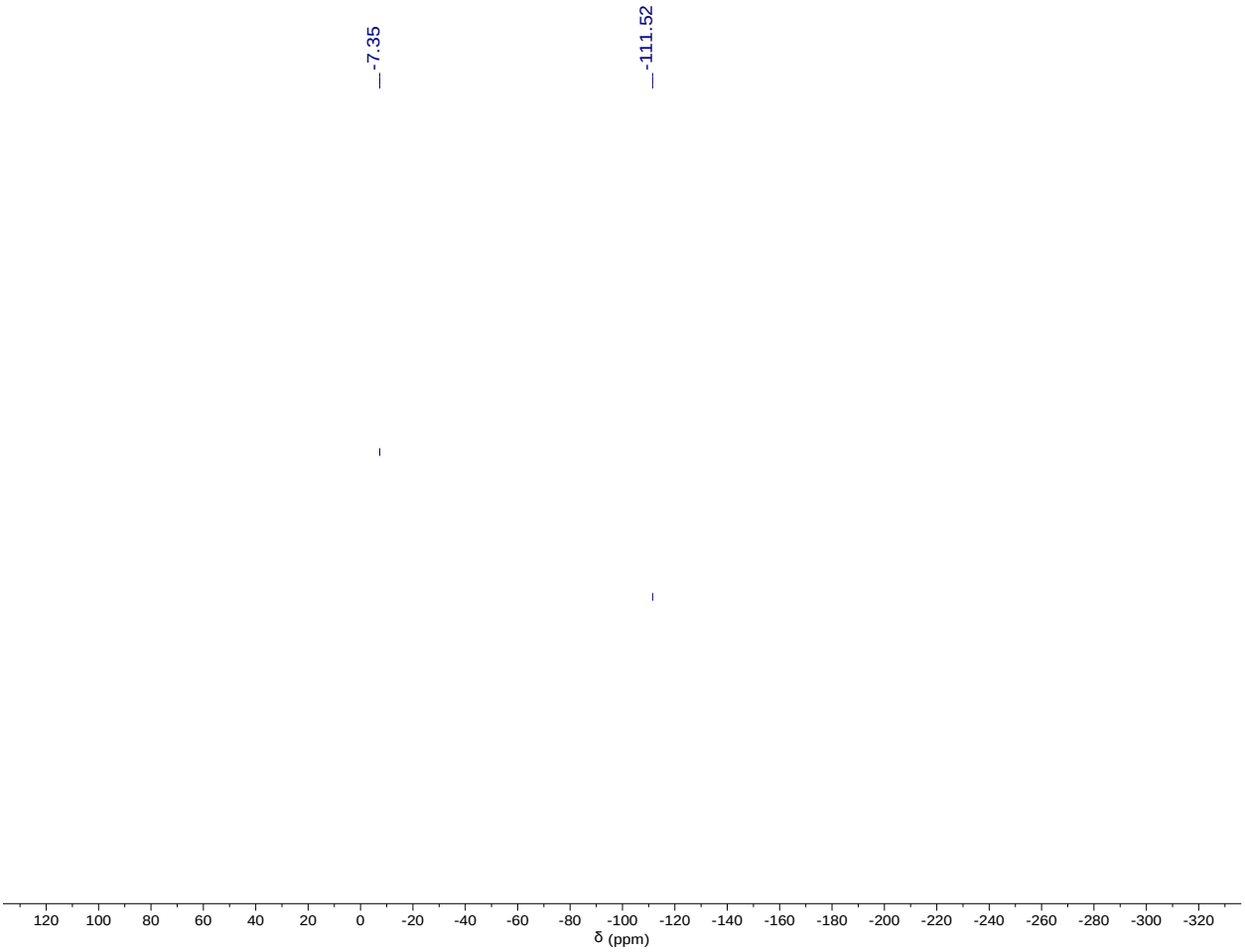

Figure S11. ^{29}Si NMR spectrum of **3** in THF-d_8. The resonance at -111.52 ppm is assignable to the borosilicate glass from the NMR tube.

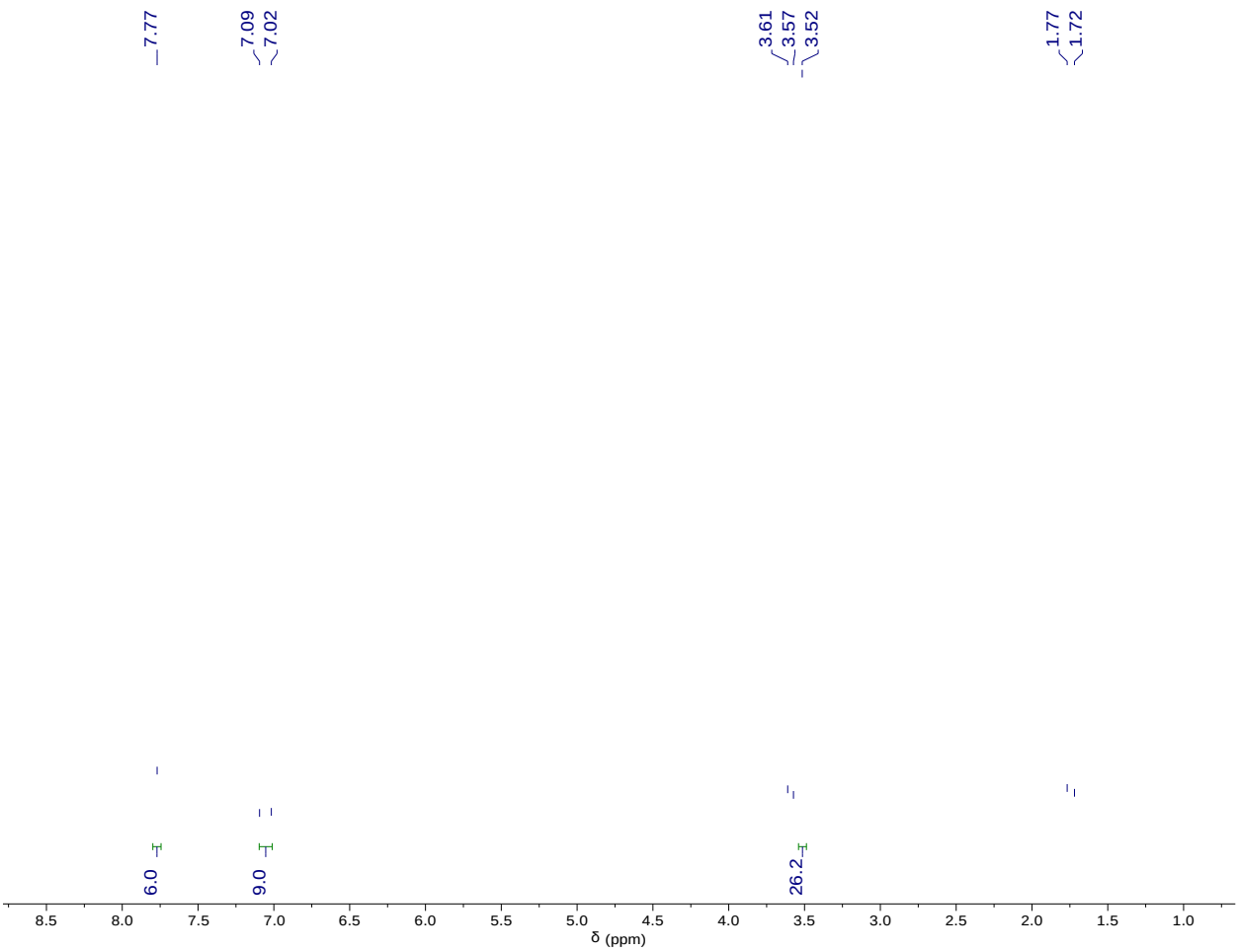

Figure S12. ^{1}H NMR spectrum of **4** in THF-d_8.

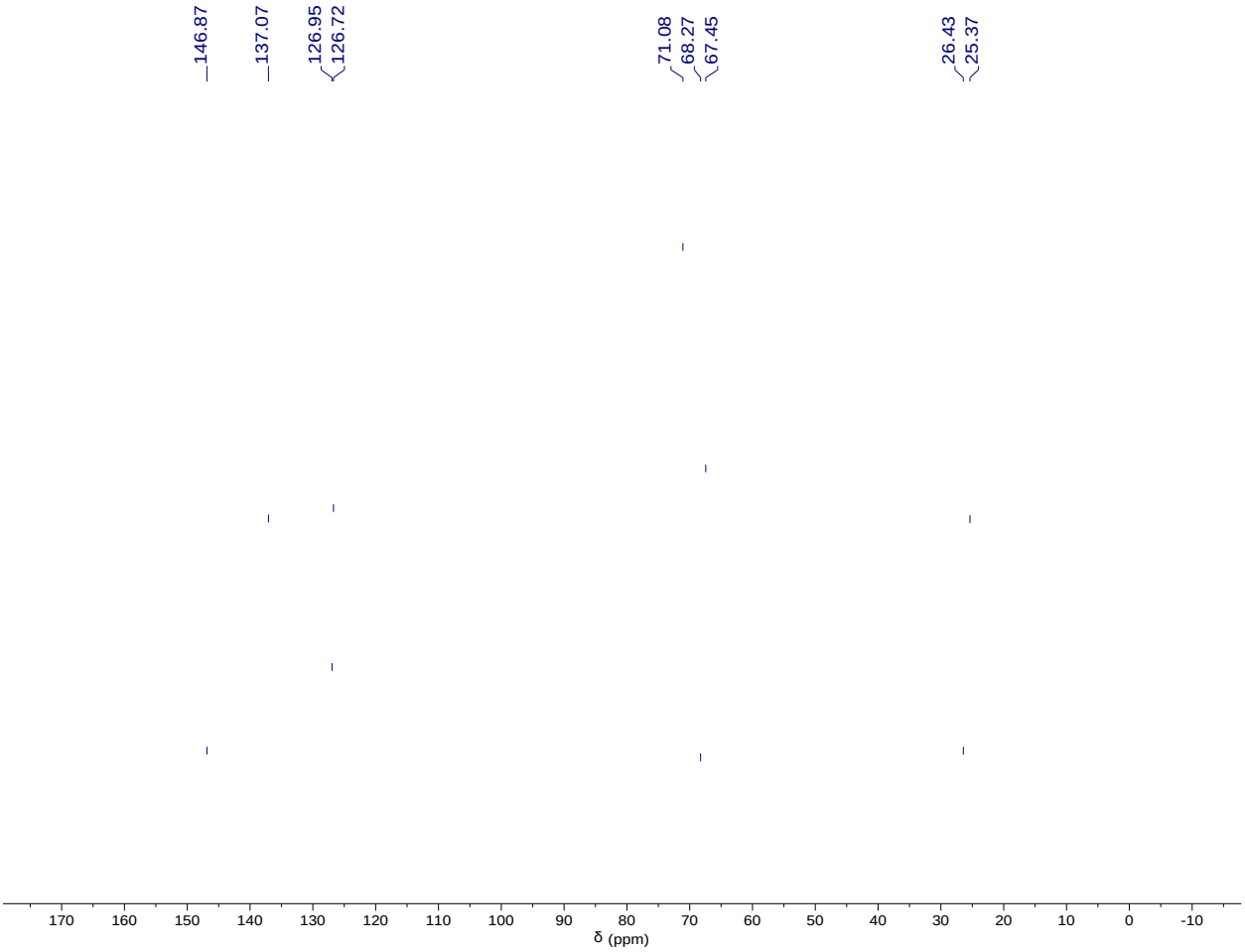

Figure S13. ^{13}C NMR spectrum of **4** in THF-d_8.

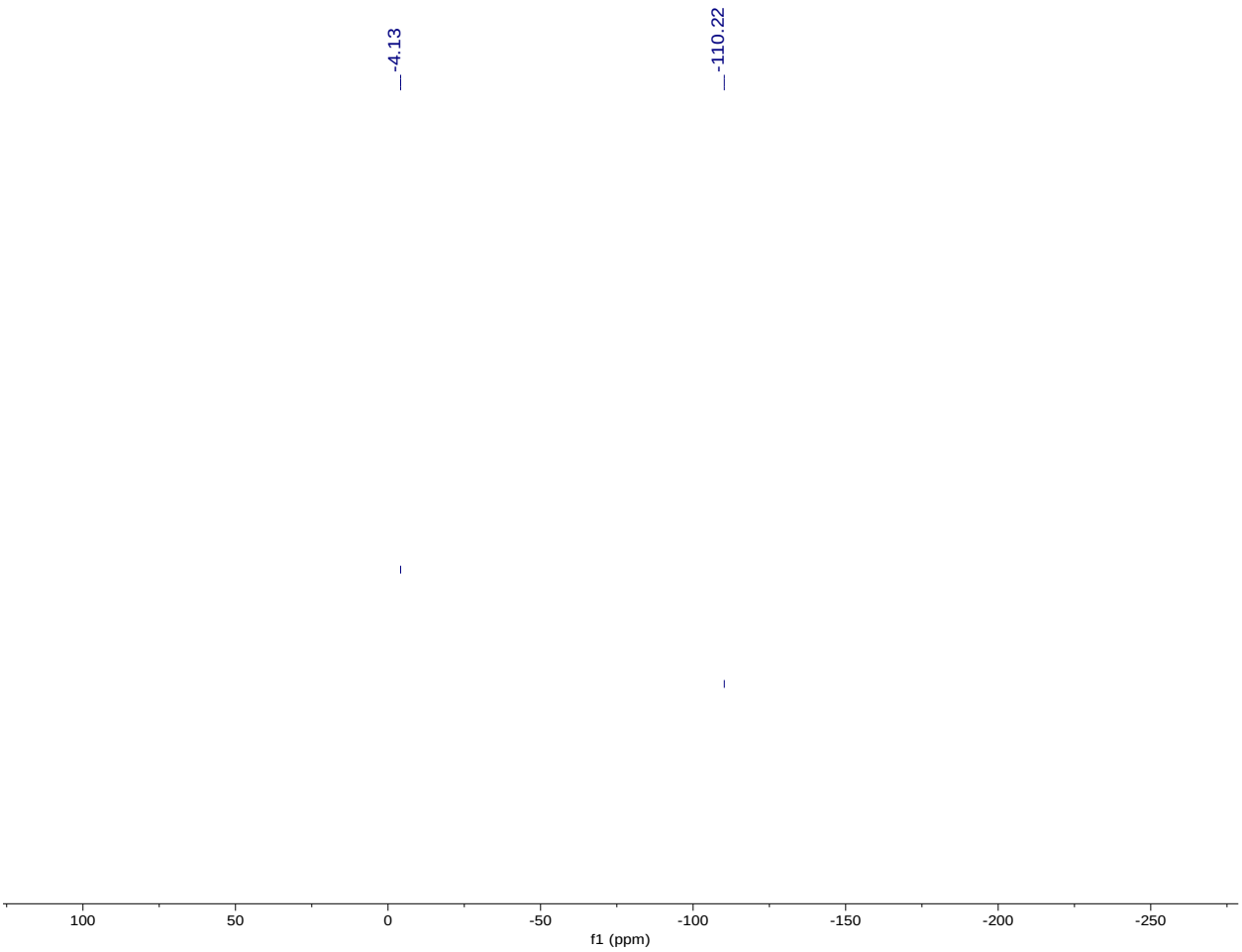

Figure S14. ^{29}Si NMR spectrum of **4** in THF-d_8. The resonance at -110.22 ppm is assignable to the borosilicate glass from the NMR tube.

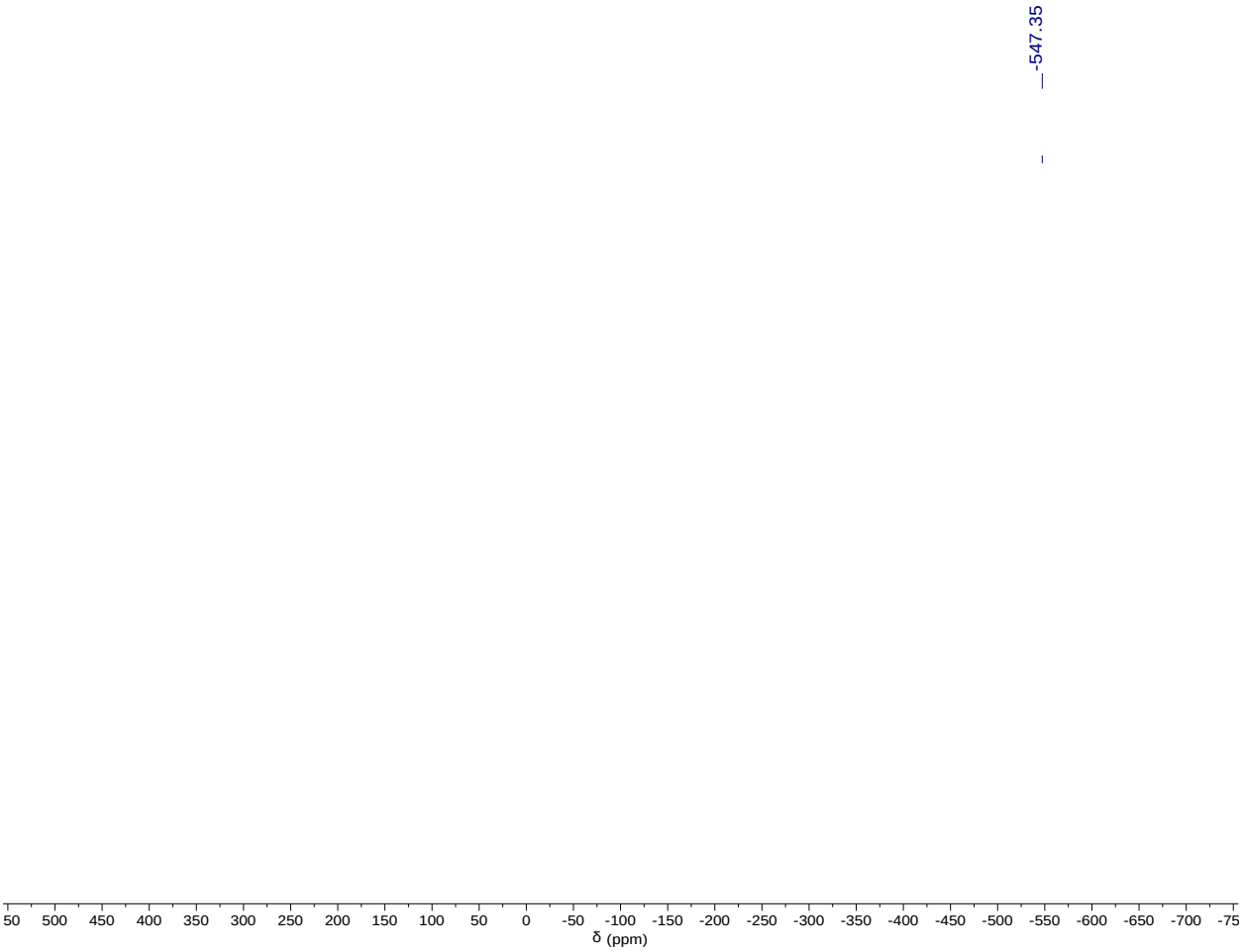

Figure S15. ^{77}Se NMR spectrum of **4** in THF-d_8.

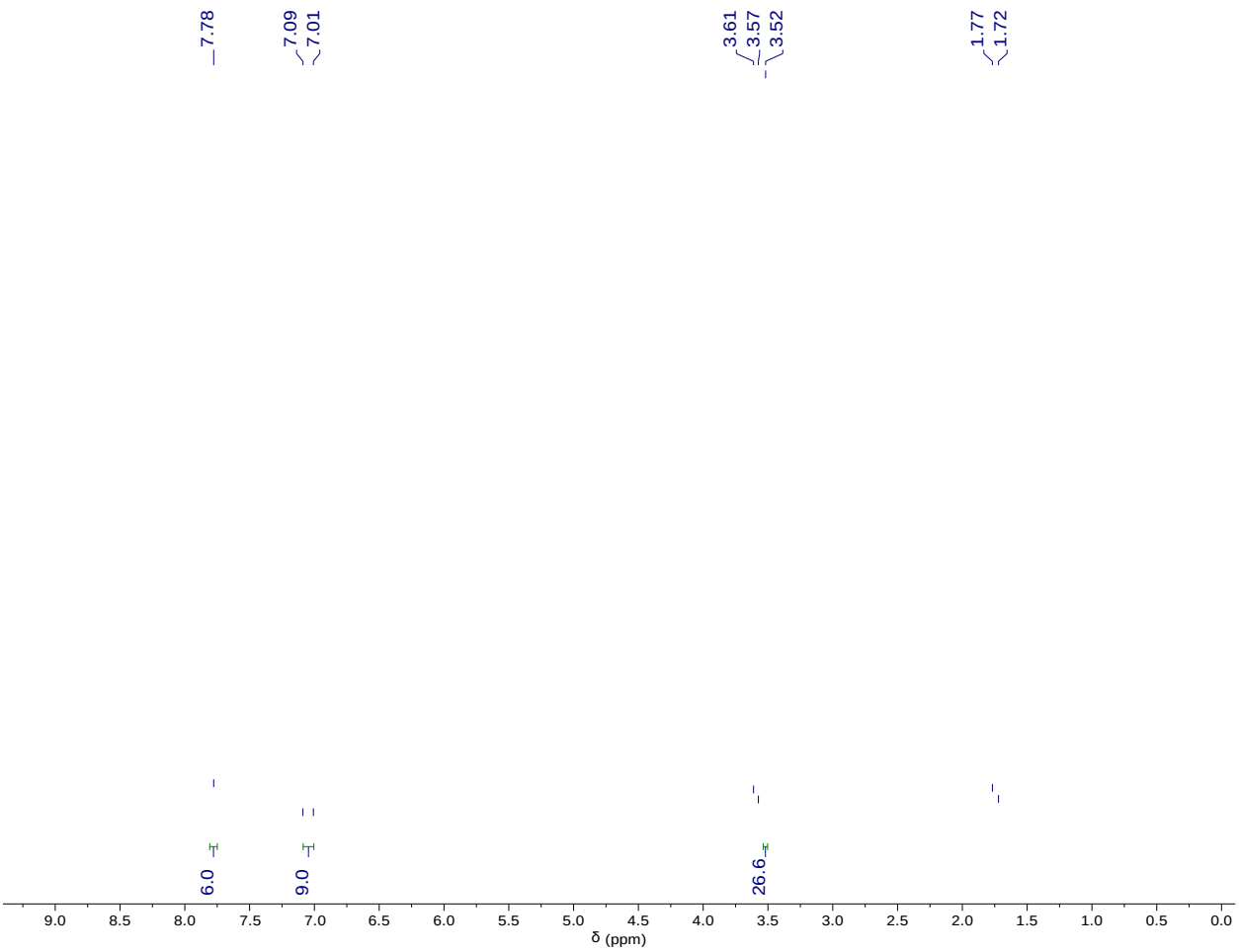

Figure S16. ^{1}H NMR spectrum of **5** in THF-d_8.

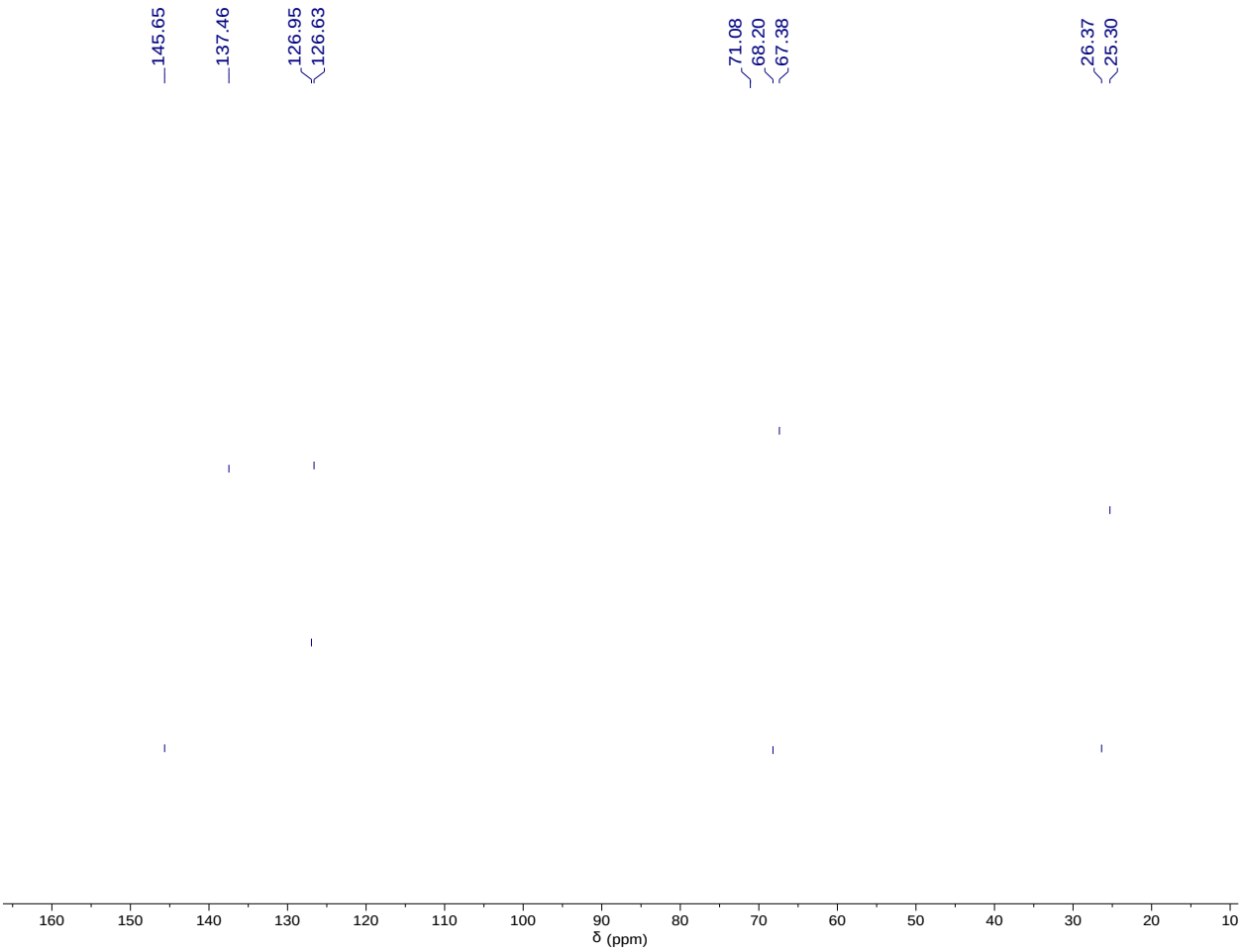

Figure S17. ^{13}C NMR spectrum of **5** in THF-d_8.

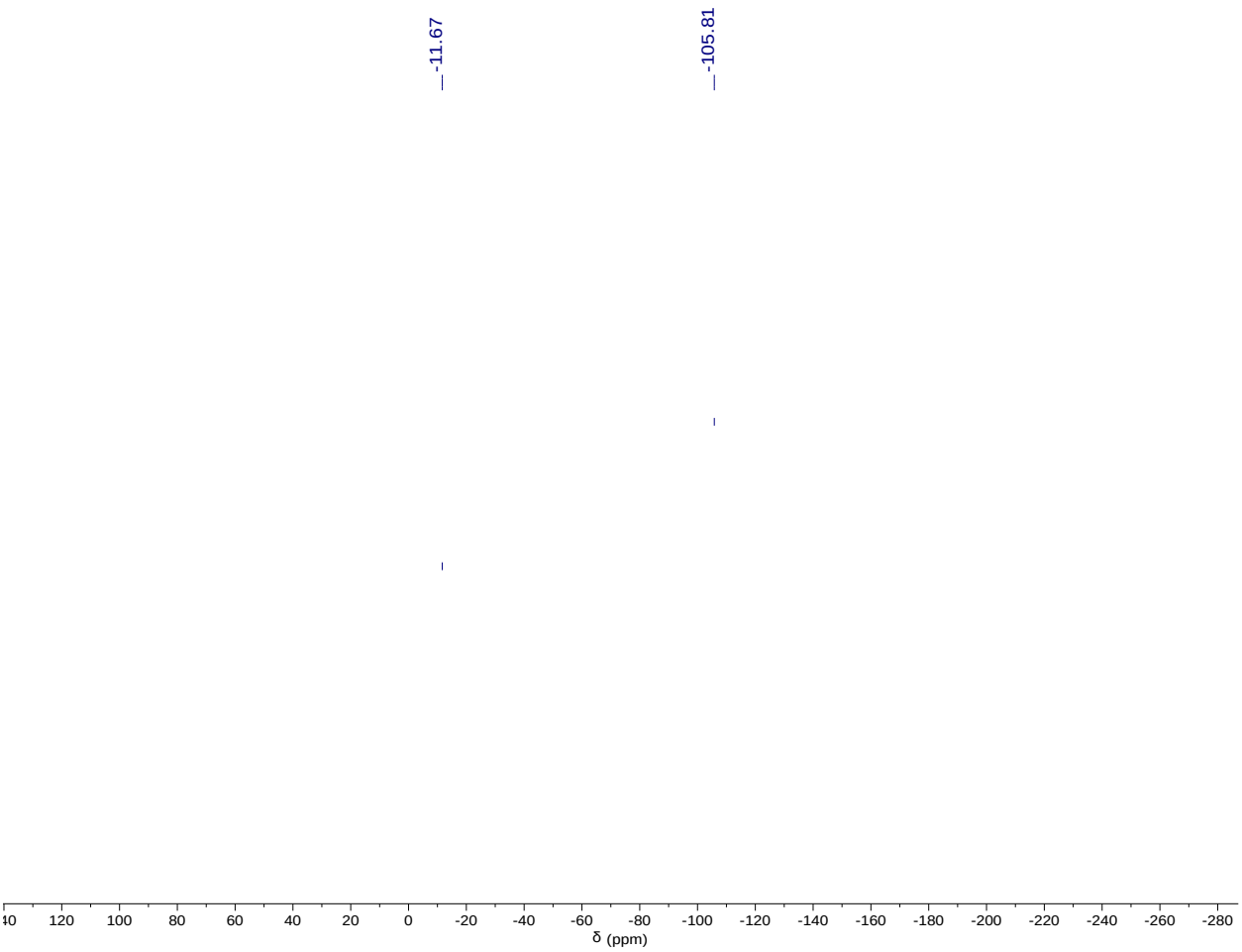

Figure S18. ^{29}Si NMR spectrum of **5** in THF-d_8. The resonance at -105.81 ppm is assignable to the borosilicate glass from the NMR tube.

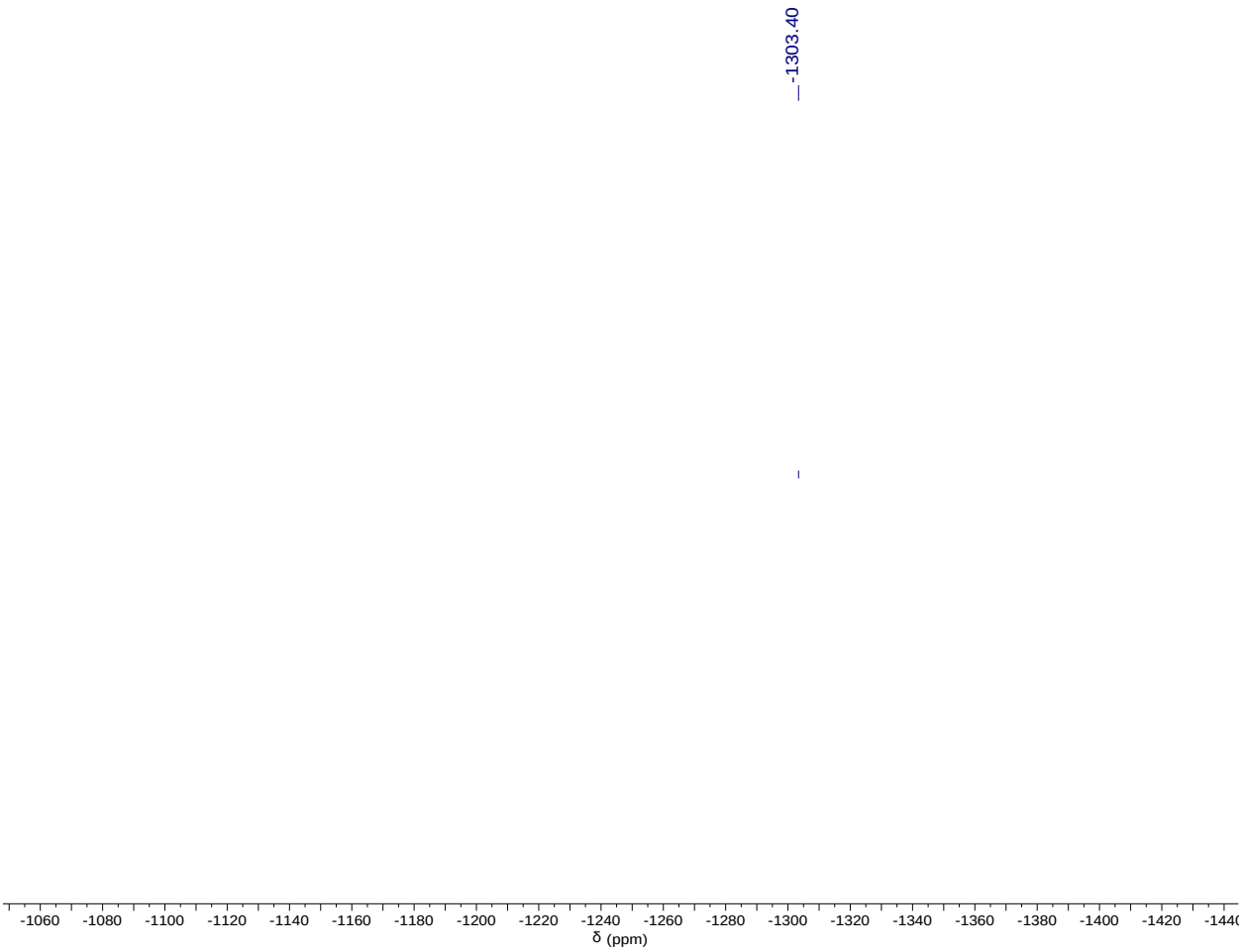

Figure S19. ^{125}Te NMR spectrum of **5** in THF-d_8.

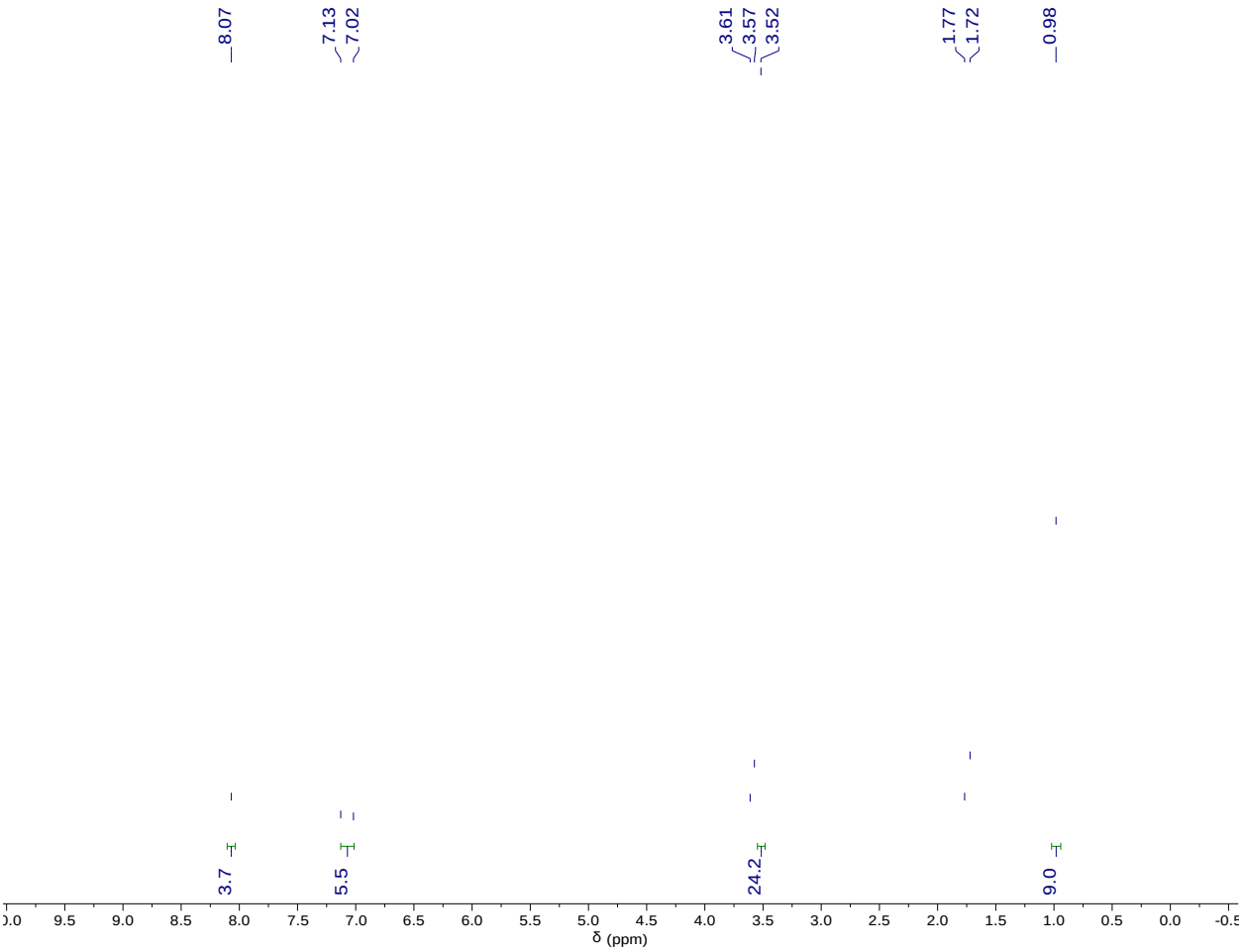

Figure S20. ^{1}H NMR spectrum of **6** in THF-d_8.

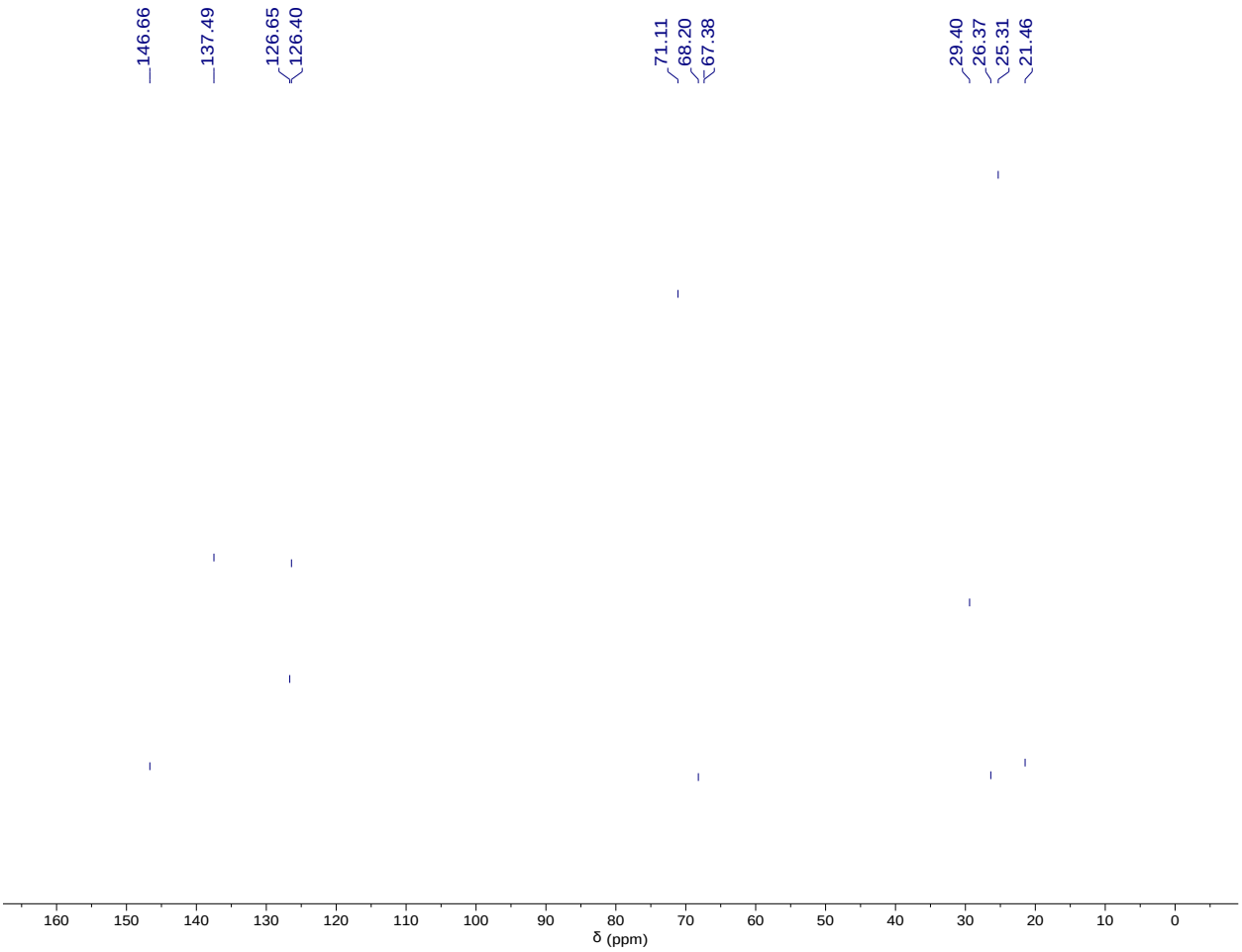

Figure S21. ^{13}C NMR spectrum of **6** in THF-d_8.

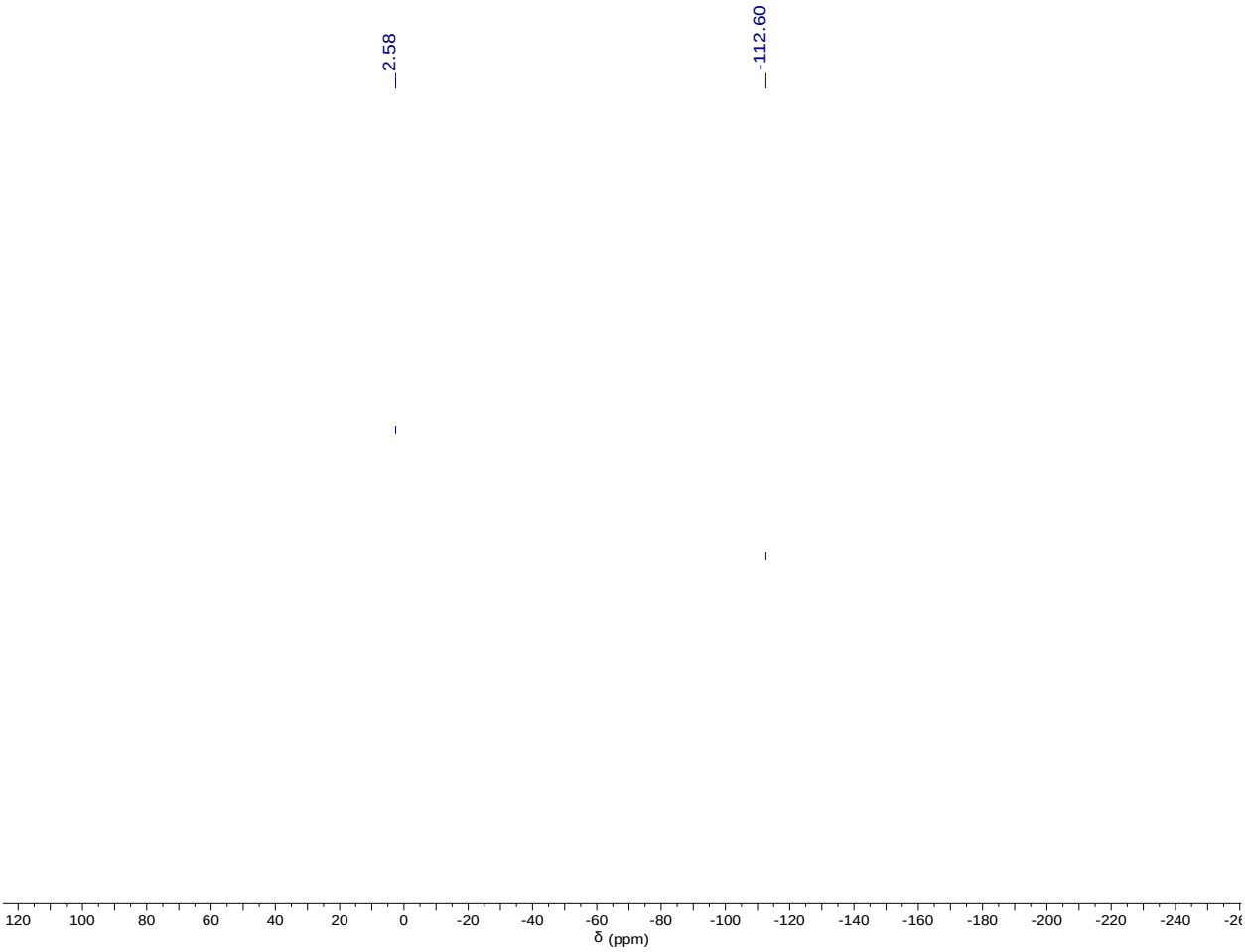

Figure S22. ^{29}Si NMR spectrum of **6** in THF-d_8. The resonance at -112.60 ppm is assignable to the borosilicate glass from the NMR tube.

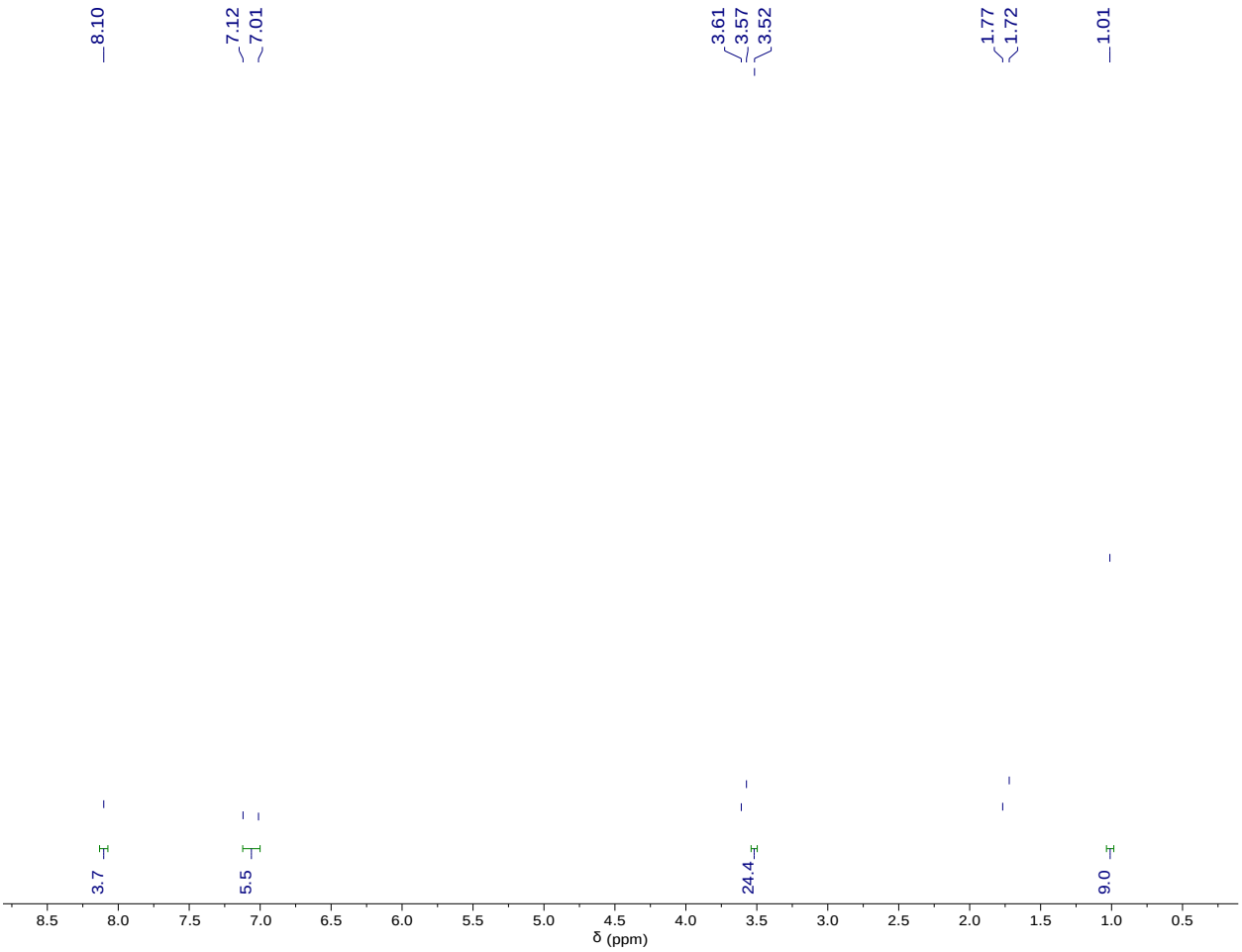

Figure S23. ^{1}H NMR spectrum of **7** in THF-d_8.

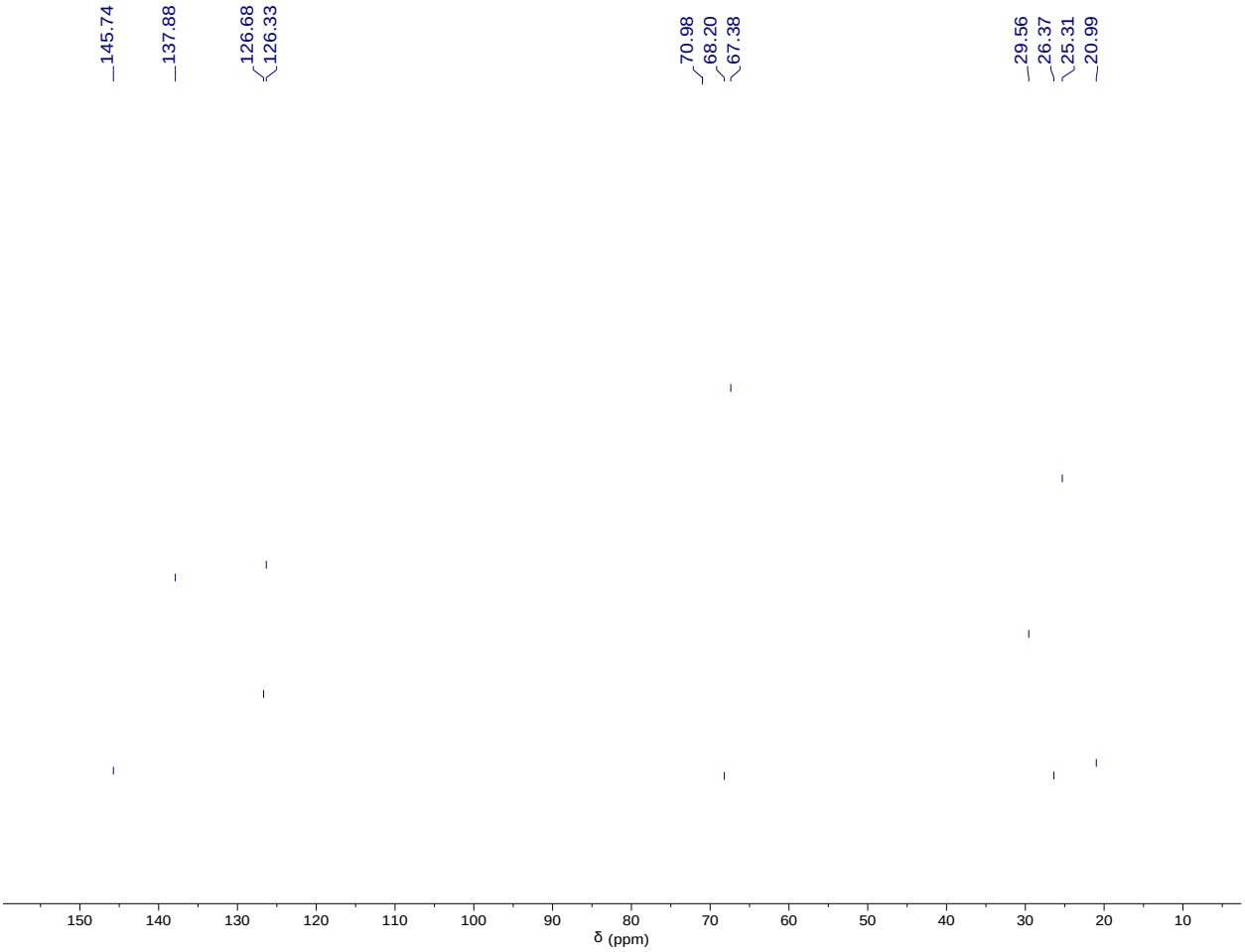

Figure S24. ^{13}C NMR spectrum of **7** in THF-d_8.

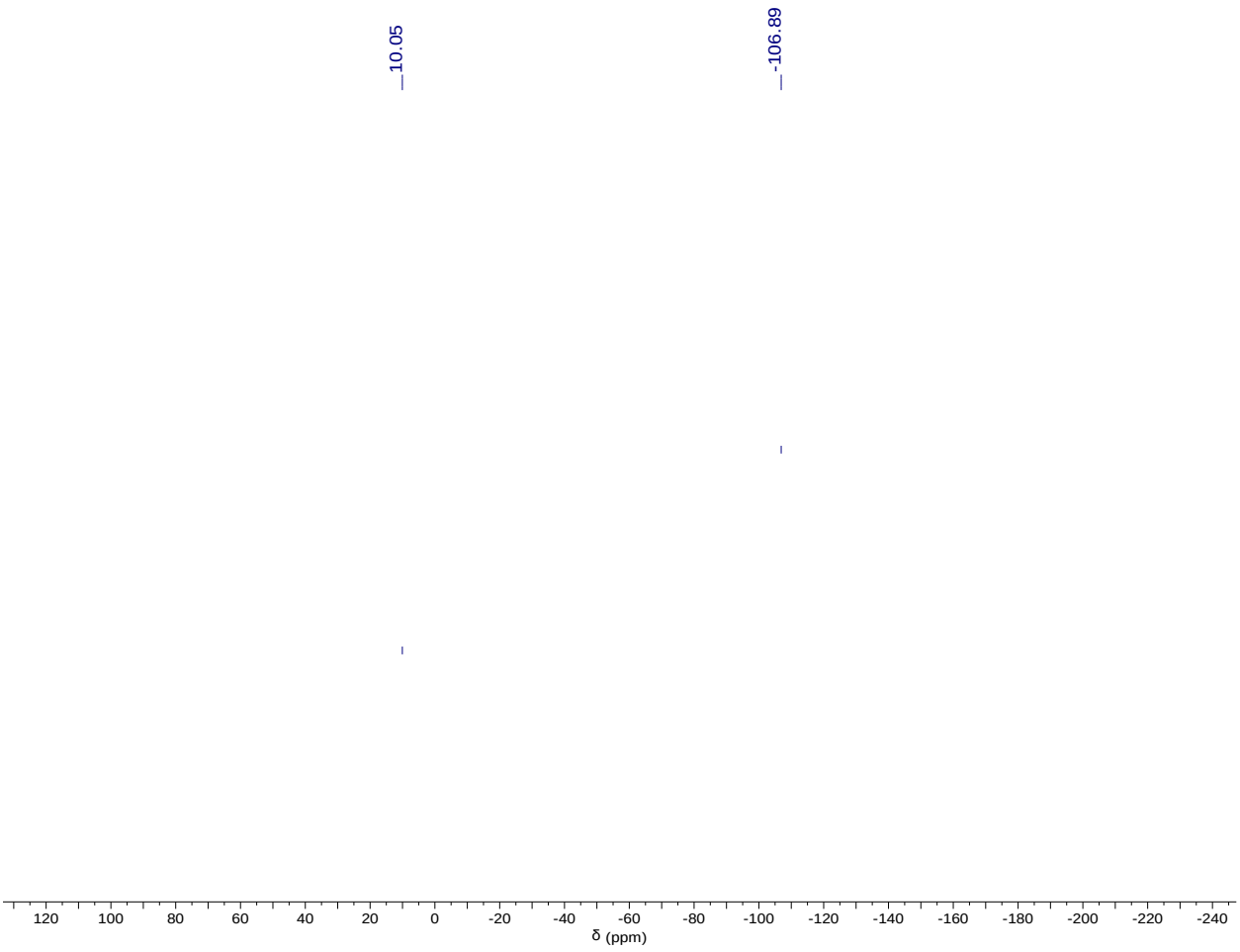

Figure S25. ^{29}Si NMR spectrum of **7** in THF-d_8. The resonance at -106.89 ppm is assignable to the borosilicate glass from the NMR tube.

Figure S26. ^{77}Se NMR spectrum of **7** in THF-d_8.

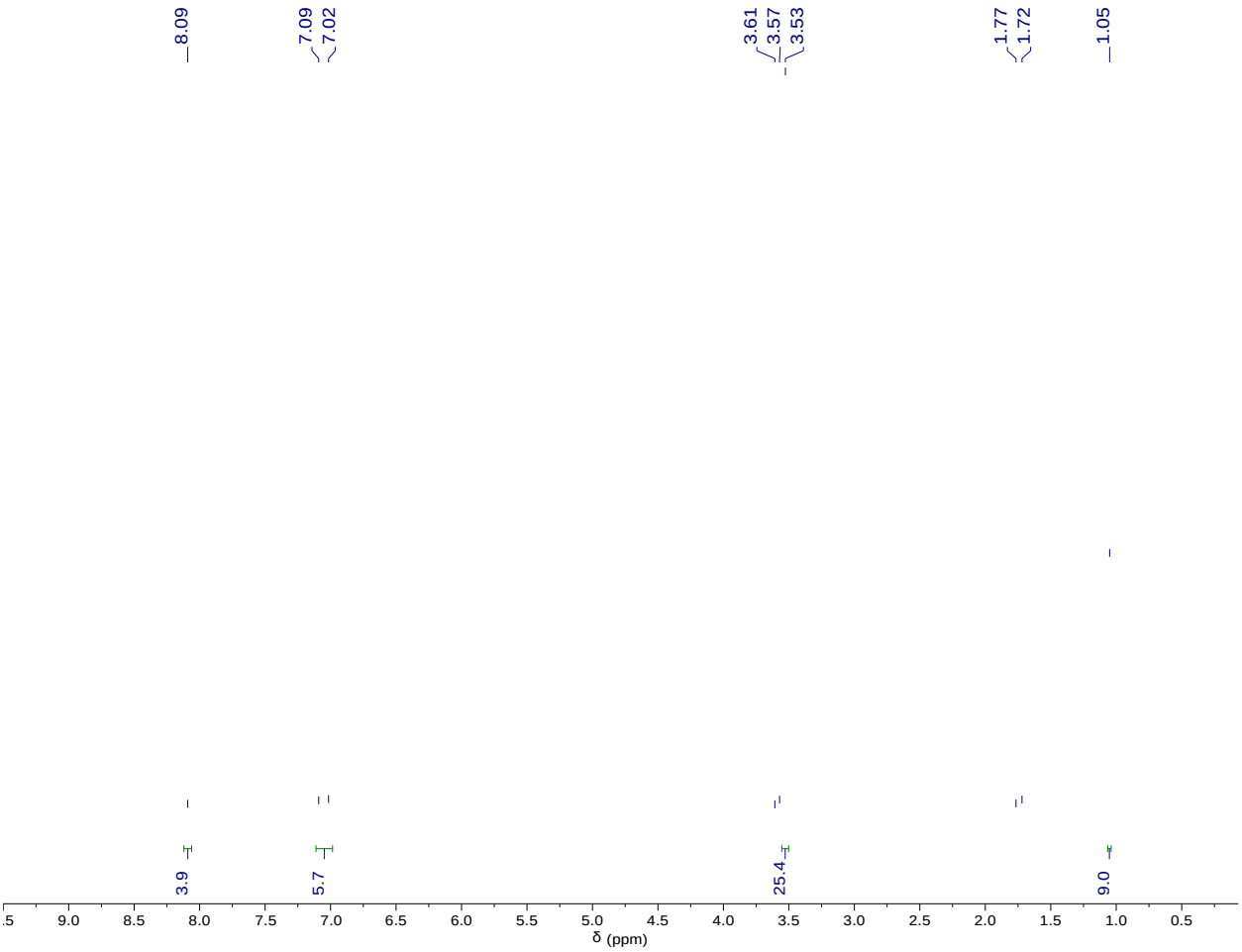

Figure S27. ^{1}H NMR spectrum of **8** in THF-d_8.

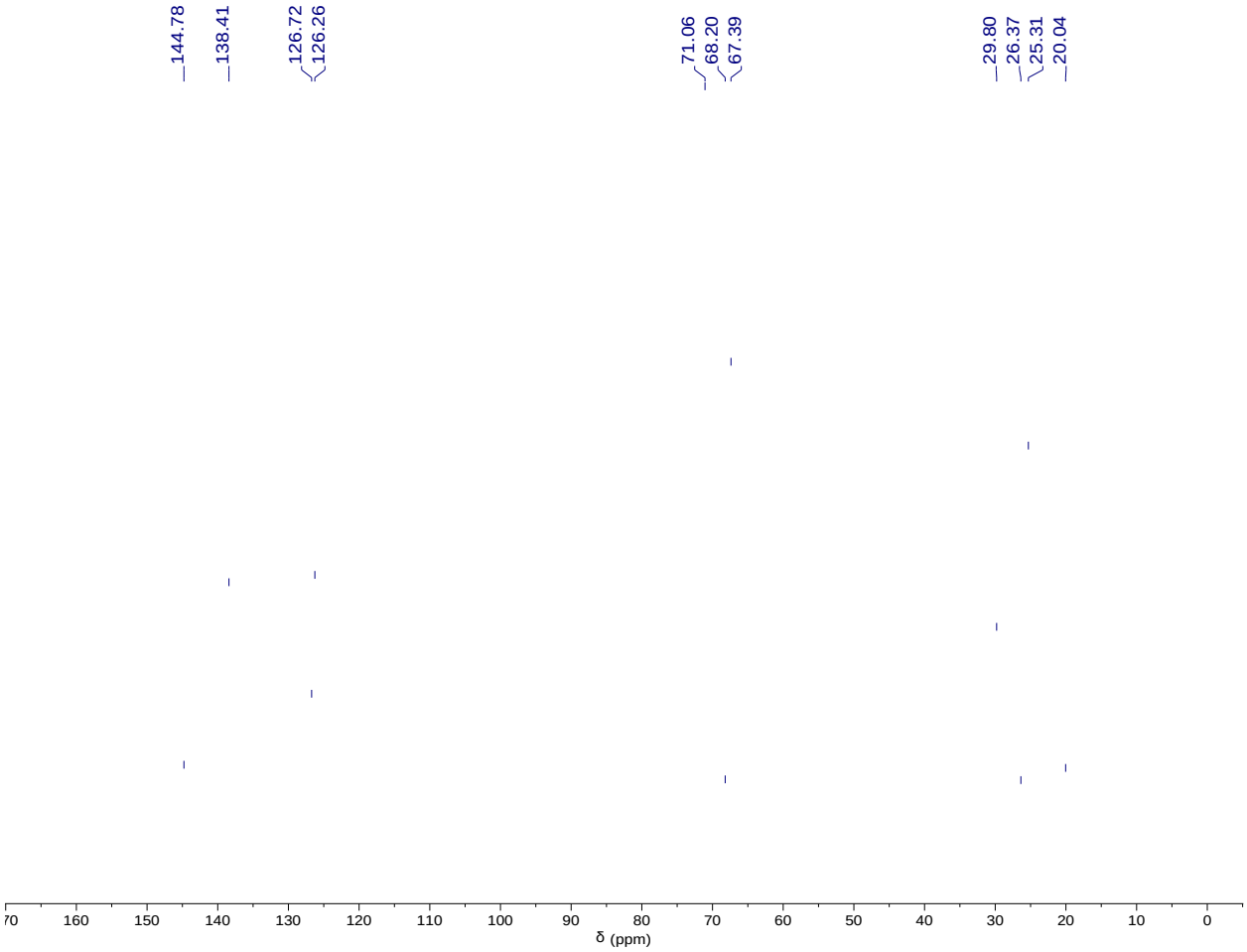

Figure S28. ^{13}C NMR spectrum of **8** in THF-d_8.

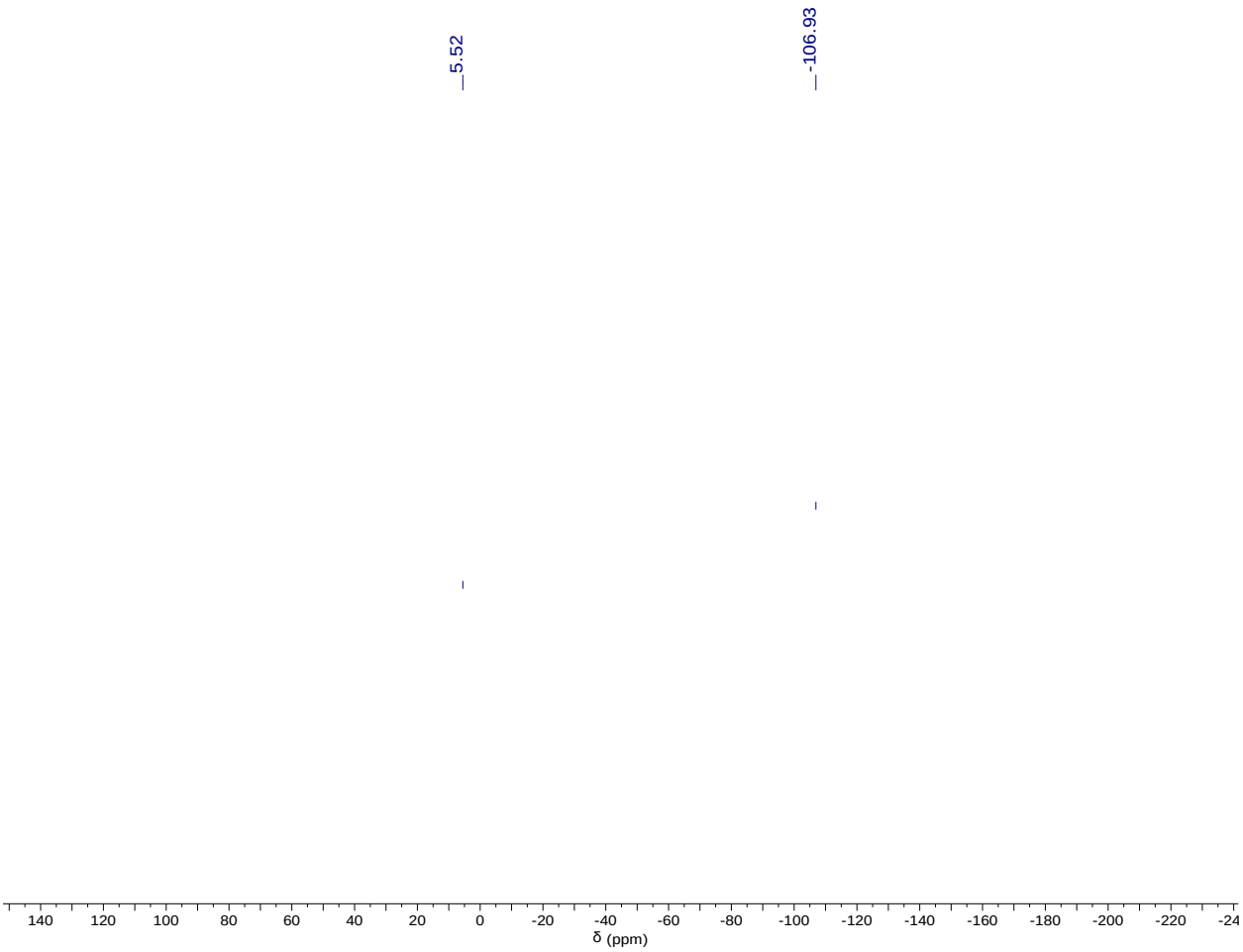

Figure S29. ^{29}Si NMR spectrum of **8** in THF-d_8. The resonance at -106.93 ppm is assignable to the borosilicate glass from the NMR tube.

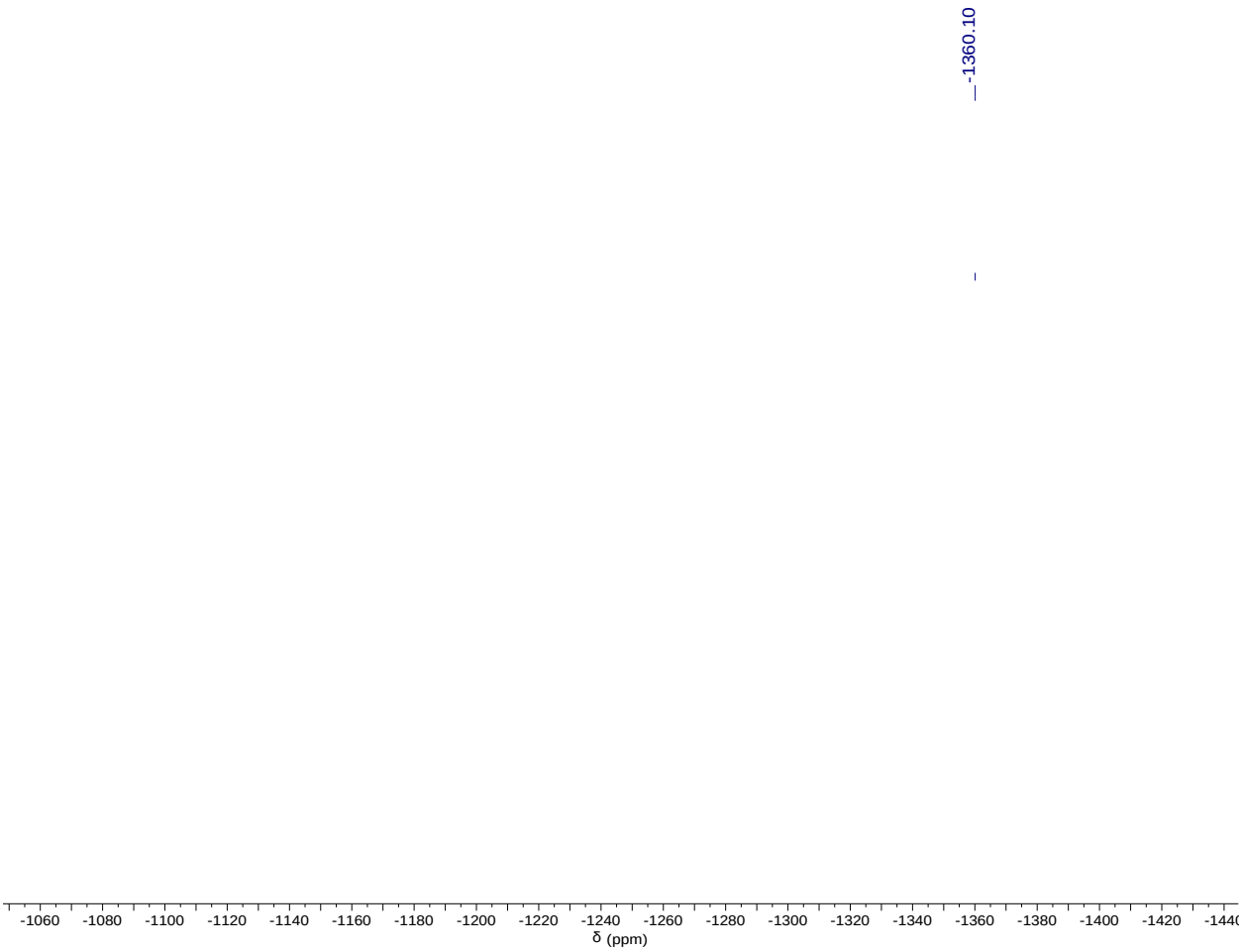

Figure S30. ^{125}Te NMR spectrum of **8** in THF-d_8.

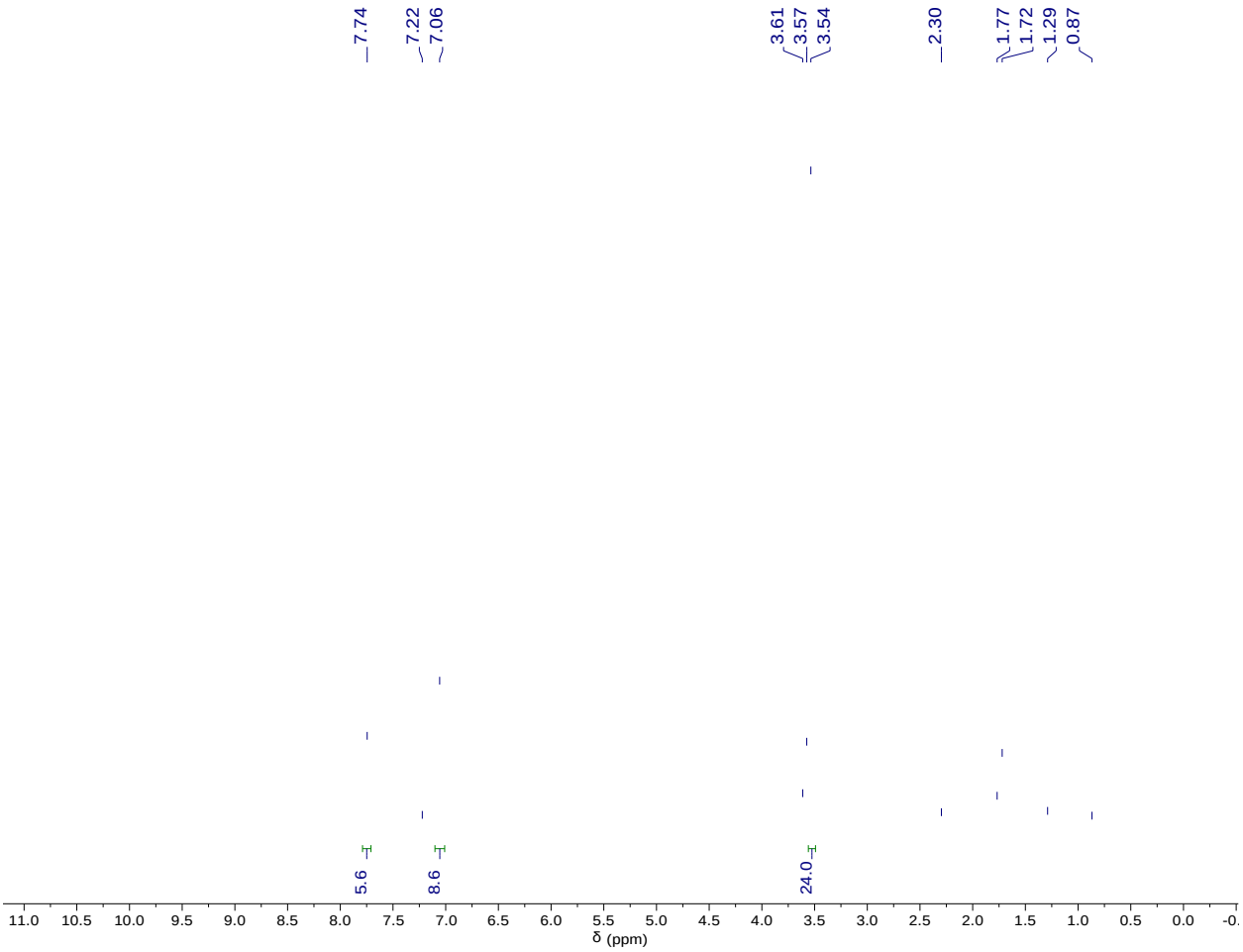

Figure 31. *In situ* ^{1}H NMR spectrum of [K(18-crown-6)][$SiPh_3$] (18.8 mg, 0.033 mmol) in THF-d_8 ~30 min after addition of 1 equiv of elemental sulfur (1.2 mg, 0.037 mmol). The resonances at 0.87 and 1.29 ppm are assignable to hexanes, while the resonances at 2.30 and 7.22 ppm are assignable to toluene.

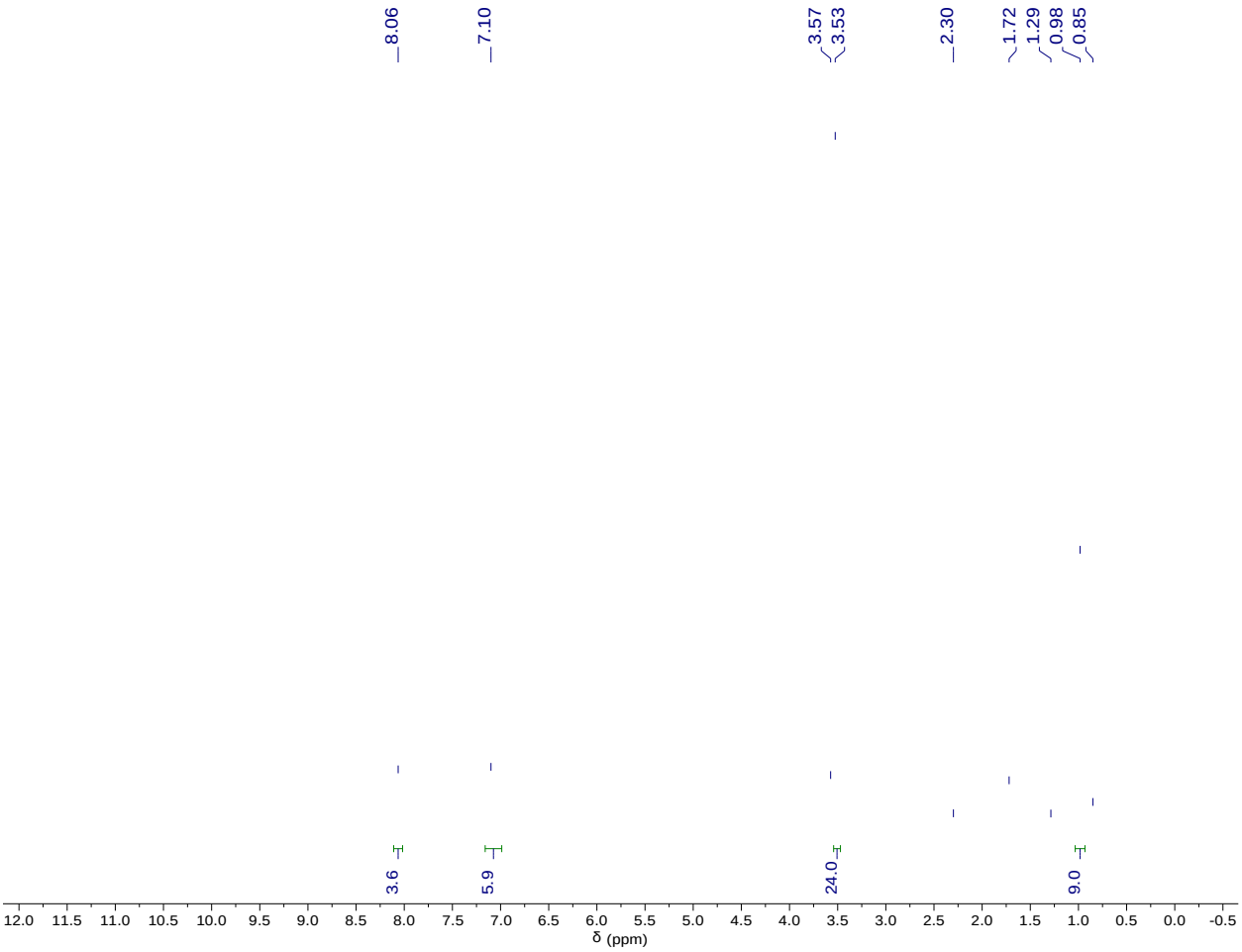

Figure 32. *In situ* ^{1}H NMR spectrum of [K(18-crown-6)][$SiPh_2{}^{t}Bu$] (23.0 mg, 0.042 mmol) in THF-d_8 ~30 min after addition of 1 equiv of elemental sulfur (1.5 mg, 0.047 mmol). The resonances at 0.85 and 1.29 ppm are assignable to hexanes, while the resonance at 2.30 is assignable to toluene.

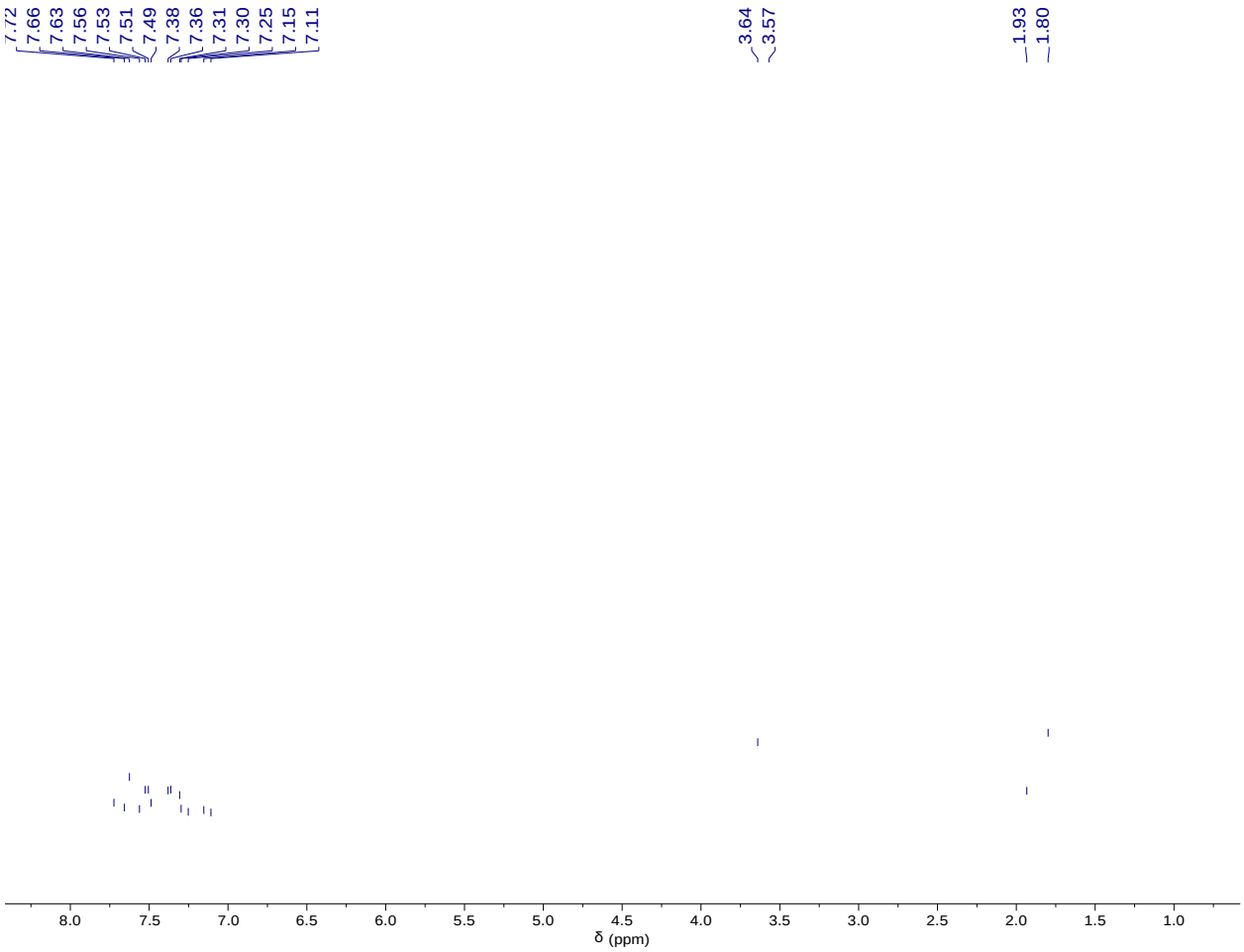

Figure 33. ^{1}H NMR spectrum of [K(18-crown-6)][$SiPh_3$] (**1**) in MeCN-d_3.The orange solid afforded a colorless solution upon dissolution into MeCN-d_3. The resonances at 1.80 and 3.64 ppm are assignable to THF. No tractable products were isolated.